

Pseudo-Bayesian Optimization

Haoxian Chen,¹ Henry Lam¹

¹ Department of Industrial Engineering and Operations Research, Columbia University

hc3136@columbia.edu, henry.lam@columbia.edu

Abstract: Bayesian Optimization is a popular approach for optimizing expensive black-box functions. Its key idea is to use a surrogate model to approximate the objective and, importantly, quantify the associated uncertainty that allows a sequential search of query points that balance exploitation-exploration. Gaussian process (GP) has been a primary candidate for the surrogate model, thanks to its Bayesian-principled uncertainty quantification power and modeling flexibility. However, its challenges have also spurred an array of alternatives whose convergence properties could be more opaque. Motivated by these, we study in this paper an *axiomatic* framework that elicits the minimal requirements to guarantee black-box optimization convergence that could apply beyond GP-related methods. Moreover, we leverage the design freedom in our framework, which we call *Pseudo-Bayesian Optimization*, to construct empirically superior algorithms. In particular, we show how using simple local regression, and a suitable “randomized prior” construction to quantify uncertainty, not only guarantees convergence but also consistently outperforms state-of-the-art benchmarks in examples ranging from high-dimensional synthetic experiments to realistic hyperparameter tuning and robotic applications.

1. Introduction

Bayesian Optimization (BO) is a popular method for the global optimization of black-box functions that are typically multimodal and expensive to evaluate. Its main idea is to model the objective landscape using observed data in order to “guess” where the global optimum is, rather than following a solution trajectory. One of the earliest works in BO is [28] in 1998, initially proposed for automotive and semiconductor designs and motivated by long runtimes of their computer codes. Nowadays, BO has been widely applied in machine learning including hyper-parameter tuning and Auto-ML [34], reinforcement learning [12], robotics [38], experimental design such as A/B testing [13], simulator calibration [3, 48], and engineering applications such as environmental monitoring [37] and aerospace system design [24]. Extensive overviews are in [10, 19, 50].

More precisely, a typical BO procedure sequentially searches for next design points to evaluate by updating a surrogate model to predict the objective and, moreover, quantify the associated uncertainty. Both the prediction and the uncertainty quantification are important as they work together, via a so-called acquisition function, to balance exploitation-exploration in the evaluation sequence. In this regard, Gaussian process (GP) has been a primary candidate of surrogate model, thanks to its Bayesian-principled uncertainty quantification power and modeling flexibility [27, 43]. However, it has a cubic-order scalability due to the inversion of the gram kernel matrix in computing the posterior and, despite its principled design, it is conceivable to construct algorithms that could leverage problem structures more efficiently. To this end, there has been a surge of active studies to improve BO. These include the sparsification of GP using pseudo-inputs [16, 25, 31, 39, 47, 51] or kernel approximation [32] to reduce its time complexity, substitution of GP with other surrogates such as random forests [26] and neural networks [45, 52, 54, 63], and most recently the direct modeling of acquisition functions over the search space instead of through a surrogate [7, 53, 57]. While these approaches provide attractive empirical enhancements, their theoretical properties become more difficult to understand due to their increased algorithmic complications. In fact,

for some of the above methods, it is known to exhibit instability issues in uncertainty quantification (see Sec.II part E in [50]) and so even the basic “consistency” of the algorithm is unclear.

Motivated by the above, we are interested in the following question: *Can we create an axiomatic framework that elicits the minimal requirements on any exploration-based algorithms to guarantee black-box optimization convergence?* To answer the above, we dissect a convergent algorithm into three independent basic ingredients, *surrogate predictor (SP)*, *uncertainty quantifier (UQ)*, and *acquisition function (AF)*. SP aims to provide point predictions at different design points. UQ quantifies the uncertainty of SP and indicates how reliable is the current prediction. AF transforms SP and UQ into the decision on which design point to evaluate next. We derive the *axiomatic* properties of SP, UQ and AF to attain theoretical convergence. In a nutshell, we call these properties *local consistency*, the *generalized no-empty-ball property*, and the *improvement property* respectively. These basic ingredients, along with our axiomatic properties, appear in GP-based algorithms – however, the main point is that GP is not the only approach that exhibits these properties; instead, there are many more algorithms that could lead to similar convergence guarantees.

The above dissection implies huge design freedom to achieve theoretical convergence. Then the next question arises: *Can we construct simple convergent algorithms that can outperform existing ones, including but not only GP-based procedures?* Fully addressing this question is conceivably intricate as it depends on specific problem instance and convergence rate analysis. However, via our axiomatic framework, we offer some empirical evidence that simple algorithms could actually outperform some existing more sophisticated procedures. To search for this simple algorithm, we go through our recipe of admissible SP, UQ and AF, and select the one with light computation and superior empirical performance. In particular, we show how combining a simple local regression as SP, a suitably constructed “randomized prior” as UQ, and expected improvement (EI) as AF, can consistently outperforms some state-of-the-art BO benchmarks across a range of numerical examples.

We call our above framework *Pseudo-Bayesian Optimization (PseudoBO)*. This is because, intuitively, we hinge on the Bayesian insight of BO in dissecting convergent procedures, but at the same time, a Bayesian perspective is generally not required for optimization convergence. Essentially, our framework extracts the minimally needed features in BO from the view of exploration-based optimization.

2. Related Works

We first review the existing literature. We categorize it roughly into two parts, one focusing on practical algorithms and implementations (Section 2.1) and one on theoretical guarantees (Section 2.2).

2.1. Literature on BO Practical Enhancements

We overview some existing approaches that aim to increase the scalability or efficiency of BO:

Sparse GP. The first approach comprises sparse pseudo-input GP [16, 25, 31, 39, 47, 51]. The idea is to select m inducing pseudo-inputs by minimizing information loss, with m smaller than number of collected data n , to reduce the rank of the involved covariance matrix and subsequently the computational complexity. The second approach is GP with sparse spectrum [32]. By Bochner’s theorem [9], the kernel can be approximated by random features and thus GP can then be approximated by Bayesian linear regression with finite basis functions of size m . In terms of complexity, both approaches reduce the time complexity from $\mathcal{O}(n^3)$ to $\mathcal{O}(nm^2 + m^3)$. However, the involved approximation and hence information loss may cause imprecise surrogate prediction or uncertainty quantification [50].

Surrogate Substitution. Rather than working on scaling GP, there has been a surge of research on replacing BO with other surrogate models. SMAC [26] leverages random forest regressor and the standard deviation among trees to quantify uncertainty. However, the uncertainty quantification from bootstrapping is unstable and can be overly small for unexplored areas. An alternative is to use neural networks for surrogate modeling. DNGO [52] adopts Bayesian linear regression on top of the the representations learnt by a neural network. Based on this, [45] proposes ABLR that improves the

two-step learning in [52] to joint Bayesian learning but with additional computational complexity. BOHAMIANN [54] uses a modified Hamiltonian Monte Carlo to improve robustness and scalability of the surrogate model. [63] uses neural network ensemble. However, they require retraining the neural network after new data is collected, which is computationally expensive. Moreover, the performance appears sensitive to the network architecture [52].

Density Ratio Estimation-based Methods. Another line of research focuses on directly modeling the acquisition function [7, 53, 57]. [7] proposes tree-structured Parzen estimator (TPE) by establishing the equivalence between expected improvement (EI) and the relative ratio between two densities, specifically for handling discrete and tree-structured inputs. Recently, BORE [57] is invented to estimate this density ratio directly with likelihood-free inference and LFBO [53] generalizes this framework to model any acquisition function in the form of expected utility.

Other Approaches. There are a variety of other works to speed up the computation of BO. One way is to leverage batch acquisition function, by proposing points in batch to be evaluated at once. Ensemble Bayesian Optimization [62] employs an ensemble of additive GPs as well as a batch acquisition function to scale BO to tens of thousands of observations. Other batch acquisition functions are proposed [14, 22, 49, 61, 64]. Another line of works focus on dimension reduction, such as BOCK [41] and HeSBO [40]. Recently, TuRBO [18] is proposed to incorporate BO with the trust region method and batch acquisition through Thompson sampling [56]. In terms of implementation, GPyTorch [20] scales GP computation to thousands of queries, with conjugate descent to solve linear systems and Lanczos process to approximate the log-determinant. By leveraging hardware development, BoTorch [4] is invented as the state-of-the-art implementation of BO, speeding up the computation of acquisition with Monte Carlo sampling, sample average approximation (SAA) and computational technologies like auto-differentiation and parallel computation on CPU and GPU.

As explained in our introduction, the above approaches are empirically attractive but most of them lack theoretical analysis. To this end, even the basic consistency, i.e., whether the algorithm converges properly or not, is not well-understood. A main goal of this work is to provide an axiomatic framework that could help supply basic theoretical convergence guarantee without expending specialized efforts into analyzing each algorithms one-by-one under specific settings. Moreover, as a by-product of our PseudoBO framework, we also investigate simple and cheap algorithms that can perform competitively against these benchmarks. Furthermore, we also note that PseudoBO is not meant to separate from the above works, in the sense that these developed tools can be combined with PseudoBO to offer better performance or accelerate the computation even more. For example, our experiments (in Section 7) include the combination with Trust Region to achieve higher scalability like in TuRBO, and the inner optimization of AF via Sobel sequence.

2.2. Literature on BO Theory

Despite the surge of methods beyond GP on the practical side, the current theory of BO is still mainly restricted to the GP paradigm and presumptions, as far as we understand. We divide the study of algorithms with theoretical guarantees into the investigation of consistency and more elaborate convergence rate analysis.

Consistency. [36] analyzes the consistency of BO with one-dimensional GP (in particular, Brownian motion) with EI. This was expanded upon [60], which extends the consistency of EI to multi-dimensional settings, assuming the GP be stationary with the inverse of its spectral density exhibiting at most polynomial growth. Later, [6] generalizes the consistency to acquisitions of both EI and knowledge gradient (KG) for any Gaussian process with continuous sample paths. Besides, consistency results have also been established in various non-standard settings. For instance, [58] considers the objective as the sum or integral of a larger number of blackbox functions whose observations can be deterministic

or noisy. [2] considers the objective with an inner network structure, where each node represents a blackbox function with deterministic output. More generally, [1] studies composite objective where a blackbox function is composited with a function that has an explicitly known structure. In the realm of simulation optimization, BO is applied to optimize an expectation-form objective function, and the simulator can possibly have the capability to generate aleatory uncertainties via common random number, e.g., [44, 65]. Additionally, [59] considers blackbox function with input parameters that are unknown but observed via external data (i.e., the so-called input uncertainty in the stochastic simulation literature, e.g., [5, 15]). It proposes Bayesian Information Collection and Optimization (BICO), which balances the trade-off between simulation and real data collection.

Convergence Rate Analysis. This is cast commonly in the form of regret, i.e., the difference between the attained objective value and the oracle best objective value attained by the unknown ground-truth solution. [55] derives the first sub-linear cumulative regret in the noisy setting for UCB acquisition. [11] analyzes the simple regret for the EGO algorithm in the deterministic setting. [29, 46] develop Bayesian regret bounds for Thompson sampling. Recently, [35] establishes a regret bound for UCB when the objective belongs to a parametric family of functions, and [33] gives a concentration bound especially when using ϵ -greedy procedures in radial basis function interpolations.

Except the recent works [35] and [33], the above literature on theoretical guarantees rely on assumptions pertinent to GP, which typically involves reproducing kernel Hilbert space that can be difficult to interpret in practice. Compared to all these works, our framework develops the dissection and axiomatic requirement on *general* algorithms and we only require continuity of the objective function.

3. Theory of Pseudo-Bayesian Optimization

Suppose we are interested in solving the optimization problem $\max_{x \in \mathcal{X}} f(x)$, where the objective function $f: \mathcal{X} \rightarrow \mathbb{R}$ is unknown and $\mathcal{X} \subset \mathbb{R}^d$ is the decision space. The observations are deterministic. To introduce PseudoBO, we start with a simple but general algorithmic framework as follows. We optimize f by using sequential function evaluations, where selecting which point to evaluate next is guided by some *evaluation worthiness (EW)* measure, say $W_n(x; \mathcal{D}_n)$. Here, n is the step index in the procedure, and $\mathcal{D}_n = \{(x_1, f(x_1)), \dots, (x_n, f(x_n))\}$ denotes the collected data up to the n -th step. For convenience, we also denote $X_n = \{x_1, \dots, x_n\}$. In PseudoBO, at each step n we solve $\max_{x \in \mathcal{X}} W_n(x; \mathcal{D}_n)$ and the solution x_{n+1} is set as the next point to evaluate. Thus, in summary, the PseudoBO algorithm is:

For each iteration $n = 1, 2, \dots, T$:
 Evaluate $f(x_n)$;
 Update $W_n(x; \mathcal{D}_n)$;
 Set $x_{n+1} \in \operatorname{argmax}_{x \in \mathcal{X}} W_n(x; \mathcal{D}_n)$.

The estimated optimal solution at any step n is $\hat{x}_n^* \in \operatorname{argmax}_{x \in X_n} f(x)$ which gives the maximum evaluated function value so far.

3.1. Basic Algorithmic Consistency

Our first result characterizes the algorithmic consistency of PseudoBO. We denote $Z^* = \max_{x \in \mathcal{X}} f(x)$ as the optimal value of the target problem, $\Delta(x, S) = \min_{y \in S} \|x - y\|$ as the set distance from $x \in \mathcal{X}$ to the set $S \subset \mathcal{X}$, and $E_f(S) = \{(x, f(x)) : x \in S\}$ as the set of evaluated pairs $(x, f(x))$ for all $x \in S$.

Assumption 3.1 (Generalized no-empty-ball property). $W_n(\cdot; \cdot)$ satisfies the following:

1. For any $x \in \mathcal{X}$, real sequence $x_n \in \mathcal{X}$ and set sequence $S_n \subset \mathcal{X}$, if $\inf_n \Delta(x, S_n \cup X_n) > 0$, where $X_n = \{x_1, \dots, x_n\}$, then $\liminf_{n \rightarrow \infty} W_n(x; A_n \cup \mathcal{D}_n) > 0$, where $\mathcal{D}_n = \{(x_1, f(x_1)), \dots, (x_n, f(x_n))\}$ and $A_n = E_f(S_n)$.

2. For any convergent sequence $x_n \in \mathcal{X}$ (i.e., $x_n \rightarrow x'$ for some $x' \in \mathcal{X}$), we have $W_n(x_n; A_{n-1} \cup \mathcal{D}_{n-1}) \rightarrow 0$, where $\mathcal{D}_{n-1} = \{(x_1, f(x_1)), \dots, (x_{n-1}, f(x_{n-1}))\}$ and $A_n = E_f(S_n)$ for any set sequence $S_n \subset \mathcal{X}$.

Roughly speaking, the first part of Assumption 3.1 stipulates that as long as there is no infinitesimally close evaluated point in the neighborhood of x , then the EW of x is positive. The second part plays a converse role that if x entails an approaching sequence, then the EW of x would shrink to 0, and this is true with or without any additional data represented by the set sequence $\{A_n\}$. Note that Assumption 3.1 is purely about the function W_n and its interaction with f , and does not assume anything about the optimization procedure. We call Assumption 3.1 the *generalized no-empty-ball (GNEB)* property, to indicate that a zero value of W_n at a point x essentially means that any ball surrounding x must contain some evaluated points in the past data, and vice versa. It is “generalized” because it extends the NEB property in [60] to allow for the incorporation of any additional information $\{A_n\}$. Moreover, note that we allow W_n to be step-dependent, i.e., depend on step n , but in many cases we can choose a W that is independent of steps.

We introduce our first theoretical result: As long as the EW W satisfies the GNEB property, PseudoBO asymptotically reaches the true optimal value, or in other words it is *algorithmically consistent*.

Theorem 3.2 (Algorithmic consistency of PseudoBO). *Suppose EW W_n satisfies Assumption 3.1 and \mathcal{X} is compact. Then \mathcal{X} is eventually populated. Consequently, if f is continuous, then PseudoBO is algorithmically consistent, i.e., the estimated optimal solution $\hat{x}_n^* \in \operatorname{argmax}_{x \in X_n} f(x)$ satisfies $f(\hat{x}_n^*) \rightarrow Z^*$ as $n \rightarrow \infty$.*

Theorem 3.2 reveals the exploration-based nature of PseudoBO: It achieves convergence by populating the search space, and while EW can incorporate many sources of information, a requirement is that it must contain information about the local popularity to guide us in this space popularization. In reality, we would like to make guesses and evaluate at points that are likely close to the best (exploitation), but also be cautious about missing out other potentially good regions (exploration). Accounting for this tradeoff requires a more specialized framework that contains ingredients to handle this issue more explicitly. We will describe these ingredients in the next subsection.

3.2. A More Specialized Framework

We consider a more specialized version of PseudoBO that materializes EW via three ingredients: *surrogate predictor (SP)*, *uncertainty quantifier (UQ)* and *acquisition function (AF)*. As discussed earlier, these ingredients appear in GP-based algorithms in BO but could be substantially more generally. Each of these ingredients needs to satisfy its own basic, independent, assumption, which we call *local consistency*, *GNEB* (introduced before) and the *improvement property* respectively.

Assumption 3.3 (Local consistency of SP). *The SP $\hat{f}(\cdot; \cdot) : \mathcal{X} \times E_f(\mathcal{X}) \rightarrow \mathbb{R}$ satisfies that for any convergent sequence $\{x_n\} \subset \mathcal{X}$, i.e., $x_n \rightarrow x'$ for some $x' \in \mathcal{X}$, we have $\hat{f}(x_n; A_{n-1} \cup \mathcal{D}_{n-1}) \rightarrow f(x')$, where $\mathcal{D}_{n-1} = \{(x_1, f(x_1)), \dots, (x_{n-1}, f(x_{n-1}))\}$ and $A_n = E_f(S_n)$ for any set sequence $S_n \in \mathcal{X}$.*

In Assumption 3.3, $\hat{f}(x; D)$ represents the predictor at x using data D . This assumption stipulates that the true function value at a target point can be approximated with increasing precision by \hat{f} constructed at evaluation points converging to this target, with the historically evaluated points and any additional data.

Assumption 3.4 (GNEB property of UQ). *The UQ $\hat{\sigma}(\cdot; \cdot) : \mathcal{X} \times E_{\hat{f}}(\mathcal{X}) \rightarrow \mathbb{R}$ satisfies:*

1. For any $x \in \mathcal{X}$, real sequence $x_n \in \mathcal{X}$ and set sequence $S_n \subset \mathcal{X}$, if $\inf_n \Delta(x, S_n \cup X_n) > 0$, where $X_n = \{x_1, \dots, x_n\}$, then $\liminf_{n \rightarrow \infty} \hat{\sigma}(x; A_n \cup \mathcal{D}_n) > 0$, where $\mathcal{D}_n = \{(x_1, f(x_1)), \dots, (x_n, f(x_n))\}$ and $A_n = E_f(S_n)$.
2. For any convergent sequence $x_n \in \mathcal{X}$, i.e., $x_n \rightarrow x'$ for some $x' \in \mathcal{X}$, we have $\hat{\sigma}(x_n; A_{n-1} \cup \mathcal{D}_{n-1}) \rightarrow 0$, where $\mathcal{D}_{n-1} = \{(x_1, f(x_1)), \dots, (x_{n-1}, f(x_{n-1}))\}$ and $A_n = E_f(S_n)$ for any set sequence $S_n \subset \mathcal{X}$.

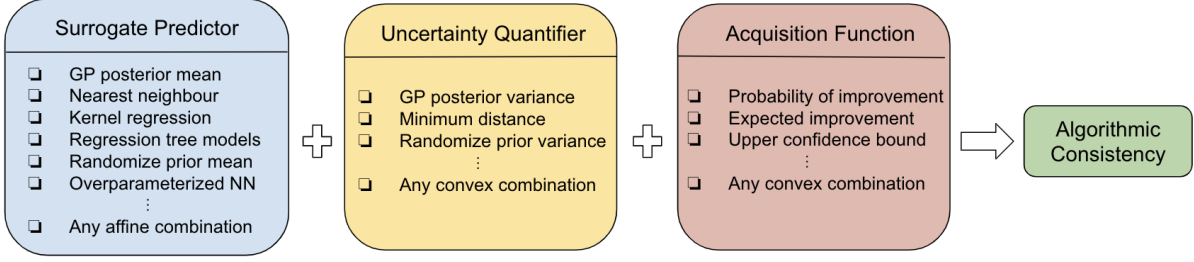


Fig. 1. A general recipe of configuring a PseudoBO algorithm.

Note that the GNEB property in Assumption 3.4 on the UQ is exactly the same as Assumption 3.1. This highlights the key role of UQ as the driver of exploration and ultimately solution convergence via the EW framework. However, by incorporating the SP via the AF (discussed momentarily), we can induce exploitation to enhance practical performances.

Assumption 3.5 (Improvement property of AF). *The AF $g_n(\cdot, \cdot) : \mathbb{R} \times \mathbb{R} \rightarrow \mathbb{R}$ satisfies the following (where p_n and q_n are any real sequences):*

1. $g_n(p_n, q_n) \rightarrow 0$ if $\limsup_{n \rightarrow \infty} p_n \leq 0$ and $q_n \rightarrow 0$.
2. $\liminf_{n \rightarrow \infty} g_n(p_n, q_n) > 0$ if $\liminf_{n \rightarrow \infty} q_n > 0$.

AF can be viewed as a channel to convert SP and UQ into EW. That is, the higher is the output of g_n is, the more worthy to evaluate is the considered point. In Assumption 3.5, p_n is the argument for the potential improvement regarding point estimation, and q_n is the argument for the uncertainty. The assumption states that if there is, with eventual certainty, no improvement, then the worthiness to evaluate is zero. In contrast, as long as there is uncertainty, then there is some worthiness to evaluate more points. Note that we allow AF to be step-dependent which is intended to make our PseudoBO framework general enough to cover common existing algorithms.

We are now ready to put together all the above ingredients into algorithmic consistency. First, for a set $\mathcal{D} \subset E_f(\mathcal{X})$, denote $\Pi_f(\mathcal{D}) = \{y : (x, y) \in \mathcal{D} \text{ for some } x \in \mathcal{X}\}$ as the projection of \mathcal{D} onto the input dimension.

Theorem 3.6 (From SP+UQ+AF to EW). *Suppose SP \hat{f} , UQ $\hat{\sigma}$, and AF g_n satisfy Assumptions 3.3, 3.4 and 3.5 respectively. Suppose also that f is continuous. Then the EW constructed by $W_n(x; \mathcal{D}_n) = g_n(\zeta(\hat{f}(x; \mathcal{D}_n) - \max \Pi_f(\mathcal{D})), \hat{\sigma}(x; \mathcal{D}_n))$, where $\zeta(\cdot)$ is continuous and increasing and $\zeta(0) \leq 0$, satisfies Assumption 3.1.*

Based on Theorems 3.2 and 3.6, we obtain the following consistency:

Corollary 3.7 (Algorithmic consistency via SP+UQ+AF). *Under the same assumptions as Theorem 3.6, for any compact \mathcal{X} , PseudoBO with EW constructed by $W_n(x; \mathcal{D}_n) = g_n(\zeta(\hat{f}(x; \mathcal{D}_n) - \max \Pi_f(\mathcal{D})), \hat{\sigma}(x; \mathcal{D}_n))$ is consistent.*

4. The PseudoBO Cookbook

We present a range of examples for SP, UQ and AF to demonstrate the generality of PseudoBO and how it applies to existing algorithms as well as new ones. Importantly, it also paves the way for us to select practically superior algorithms. Our results can be summarized as a PseudoBO recipe in Figure 1.

4.1. SP with Local Consistency

The essence of local consistency is that the SP can correctly estimate the objective value with sufficient data around, given some smoothness of the objective. An exemplifying type of locally consistent SP is

the class of interpolating models, which use the evaluated value on surrounding observed design points as the prediction. GP posterior mean, nearest neighbor, and over-parameterized neural networks and regression trees are examples. We offer a detailed description of these methods in Appendix 8.

Proposition 4.1 (Local consistency of GP’s posterior mean). *Assume a GP’s covariance function \mathcal{K} is continuous and $f \sim GP(\mu(\cdot), \mathcal{K}(\cdot, \cdot))$. Then the GP’s posterior mean is locally consistent.*

Proposition 4.2 (Local consistency of nearest neighbour). *Assume f is continuous. Then nearest-neighbor estimator is locally consistent.*

Proposition 4.3 (Local consistency of over-parameterized neural network). *Assume a neural network is differentiable, L -Lipschitz, and over-parameterized to collected data, so that it fits perfectly on training data. Assume f is continuous. Then the neural network estimator is locally consistent.*

Proposition 4.4 (Local consistency of regression tree). *Assume f is Lipschitz, and certain assumptions on regression tree’s splitting mechanism and number of samples within each leaf, then the regression tree estimator is locally consistent.*

A more formal statement on regression trees can be found in Appendix Sec. 11.

Another type of locally consistent estimators is the family of models that can have increasingly accurate estimates for points collected so far, but these estimates are not necessarily the evaluated values at any observed points. This includes, for instance, kernel regression with bandwidth decreasing at certain rate, which is defined as

$$\hat{f}(x; \mathcal{D}_n) = \sum_{i \leq n} \frac{\mathcal{K}_{h_n}(x, x_i)}{\sum_{j \leq n} \mathcal{K}_{h_n}(x, x_j) + n^{-2} \cdot \mathbb{1}\{\sum_{j \leq n} \mathcal{K}_{h_n}(x, x_j) = 0\}} f(x_i), \quad (1)$$

where h_n denotes the bandwidth at n -th iteration.

Proposition 4.5 (Local consistency of kernel regression). *Assume the kernel regression’s kernel function \mathcal{K} is shift-invariant. Additionally, if \mathcal{K} is finitely supported, then kernel regression estimator is locally consistent.*

Local consistency can be preserved if we apply any locally consistent estimator together with a “randomized prior” that we will introduce in more detail when discussing our UQ examples.

Proposition 4.6 (Local consistency of randomized prior). *Assume the regressor in the randomized prior method is locally consistent, and the prior function is sampled from a continuous random field, then the mean of the randomized prior method is locally consistent.*

Moreover, as a meta-approach, if we have a class of locally consistent estimators, then their affine combination will also enjoy local consistency.

Proposition 4.7 (Local consistency of hybrid SP). *Given a set of locally consistent SPs $\hat{\mathcal{F}} := \{\hat{f}_1, \hat{f}_2, \dots\}$, the hybrid SP $\sum_{i=1}^{|\hat{\mathcal{F}}|} \alpha_i \hat{f}_i$, where $\sum_{i=1}^{|\hat{\mathcal{F}}|} \alpha_i = 1$, is locally consistent.*

4.2. UQ with GNEB Property

GNEB in a UQ entails that the quantified uncertainty at the queried points decreases over time to 0, while it stays positive for any unexplored area. For GP posterior or simple minimum-distance measure, their UQs decrease to 0 for the queried points, but the positiveness for unexplored regions needs additional assumptions especially for the GP’s covariance function.

Proposition 4.8 (GNEB of GP’s posterior variance [60]). *Under the same assumption as in Proposition 4.1, and additionally, the GP is stationary and has spectral density \mathcal{S} , with the property that \mathcal{S}^{-1} has at most polynomial growth, then the GP posterior variance is GNEB.*

Proposition 4.9 (GNEB of minimum distance). *Δ is GNEB.*

Randomized prior is initially proposed in [42] for uncertainty quantification in deep reinforcement. Compared to the bootstrap [17], it appears procedurally similar but conceptually different. In particular, it aims to produce high uncertainty for explored or sparse regions, while the bootstrap is designed to work well only when data are sufficiently abundant. [42] proposes this method with neural network; however, we generalize it to broader regressors. Formally, with a random function $r \sim \mathcal{R}$, we can fit a random surrogate $\hat{f}_{r,n}(x_0; \mathcal{D}_n) = r(x_0) + \hat{f}(x_0; \mathcal{D}'_n)$, where \hat{f} is a locally consistent predictor fitted on data \mathcal{D}'_n with label adjusted by random function r , namely $\mathcal{D}'_n := (x_i, f(x_i) - r(x_i))_{i=1}^n$. With this, its SP and UQ can be computed as $\mathbb{E}_{r \sim \mathcal{R}}[\hat{f}_{r,n}(x_0; \mathcal{D}_n)]$ and $(\text{Var}_{r \sim \mathcal{R}}[\hat{f}_{r,n}(x_0; \mathcal{D}_n)])^{1/2}$ respectively.

Proposition 4.10 (GNEB of randomized prior’s variance). *Under the assumptions of Proposition 4.5, and in particular, using kernel regression as the locally consistent estimator in the randomized prior method, with the additional assumption that the random field has positive variance everywhere, its variance is GNEB.*

Finally, we again offer a meta-approach to combine UQs:

Proposition 4.11 (GNEB of hybrid UQ). *Given a set of GNEB UQs $\hat{\Sigma} := \{\hat{\sigma}_1, \hat{\sigma}_2, \dots\}$, the hybrid UQ $\sum_{i=1}^{|\hat{\Sigma}|} \alpha_i \hat{\sigma}_i$, where $\sum_{i=1}^{|\hat{\Sigma}|} \alpha_i = 1$ and $\alpha_i \geq 0$, is GNEB.*

4.3. AF with Improvement Property

The improvement property of AF, which signifies a zero EW for points that certainly lead to no improvement while positive for uncertain points, is satisfied by classical criteria such as probability of improvement (PI) and expected improvement (EI). To illustrate this, by using a probabilistic, specifically normal, model on $f(x)$, we obtain closed-form PI and EI as examples of AF:

$$\text{PI}(x; \mathcal{D}_n) = \begin{cases} \Phi((p(x; \mathcal{D}_n) - \tau) / \hat{\sigma}(x; \mathcal{D}_n)), & \text{if } \hat{\sigma}(x; \mathcal{D}_n) > 0, \\ \mathbb{1}\{(p(x; \mathcal{D}_n) - \tau) > 0\}, & \text{if } \hat{\sigma}(x; \mathcal{D}_n) = 0. \end{cases} \quad (2)$$

$$\text{EI}(x; \mathcal{D}_n) = \begin{cases} \hat{\sigma}(x; \mathcal{D}_n) \phi\left(\frac{p(x; \mathcal{D}_n) - \tau}{\hat{\sigma}(x; \mathcal{D}_n)}\right) + (p(x; \mathcal{D}_n) - \tau) \Phi\left(\frac{p(x; \mathcal{D}_n) - \tau}{\hat{\sigma}(x; \mathcal{D}_n)}\right), & \text{if } \hat{\sigma}(x; \mathcal{D}_n) > 0, \\ \max\{p(x; \mathcal{D}_n) - \tau, 0\}, & \text{if } \hat{\sigma}(x; \mathcal{D}_n) = 0. \end{cases} \quad (3)$$

where $p(x; \mathcal{D}_n) := \hat{f}(x; \mathcal{D}_n) - \max \Pi_f(\mathcal{D}_n)$, $\phi(\cdot)$ and $\Phi(\cdot)$ denotes the pdf and cdf of $\mathcal{N}(0, 1)$. Hyper-parameter τ can be viewed as a prescribed tolerance parameter to indicate whether the improvement is worthwhile. Then we have the following:

Proposition 4.12 (Improvement Property of PI). *With $\tau > 0$, PI defined as (2) has the improvement property.*

Proposition 4.13 (Improvement Property of EI). *With $\tau \geq 0$, EI defined as (3) has the improvement property.*

Another popular acquisition function is upper confidence bound (UCB), defined as $\text{UCB}(x; \mathcal{D}_n) = \hat{f}(x; \mathcal{D}_n) + \beta_n \hat{\sigma}(x; \mathcal{D}_n)$ where β_n is a step-dependent positive hyper-parameter to trade-off exploitation and exploration. The improvement property of UCB can be shown by rewriting the UCB expression as

$$\text{UCB}(x; \mathcal{D}_n) = \frac{p(x; \mathcal{D}_n) - \tau}{\beta_n} + \hat{\sigma}(x; \mathcal{D}_n) \quad (4)$$

This alternative expression of UCB outputs identical next point to query compared to the more familiar form, since $\arg \max_{x \in \mathcal{X}} \hat{f}(x; \mathcal{D}_n) + \beta_n \hat{\sigma}(x; \mathcal{D}_n) = \arg \max_{x \in \mathcal{X}} (\hat{f}(x; \mathcal{D}_n) - \max \Pi_f(\mathcal{D}_n) - \tau) + \beta_n \hat{\sigma}(x; \mathcal{D}_n) = \arg \max_{x \in \mathcal{X}} \frac{p(x; \mathcal{D}_n) - \tau}{\beta_n} + \hat{\sigma}(x; \mathcal{D}_n)$.

Proposition 4.14 (Improvement Property of UCB). *With $\tau \geq 0$, $\beta_n \geq 0$ and β_n strictly increasing in n , UCB defined as (4) has the improvement property.*

As for SP and UQ, we can also use a meta-approach to construct AF by combining individual ones:

Proposition 4.15 (Improvement property of hybrid AF). *Given a set of AFs with the improvement property $\mathcal{G} := \{g_1, g_2, \dots\}$, the hybrid AF $\sum_{i=1}^{|\mathcal{G}|} \alpha_i g_i$, where $\sum_{i=1}^{|\mathcal{G}|} \alpha_i = 1$ and $\alpha_i \geq 0$, has the improvement property.*

5. Grey-Box Optimization

Before we discuss how to leverage PseudoBO to search for practically superior algorithms, we digress slightly in this section to discuss how PseudoBO can be applied beyond black-box optimization. In particular, we illustrate how it can be extended to solve grey-box optimization where we know part of the objective. Formally, we unify this type of optimization tasks as

$$\max_{\tilde{x} := (x^{(1)}, \dots, x^{(u)}) \in \prod_{i=1}^u \mathcal{X}^{(i)}} F(x^{(1)}, \dots, x^{(u)}) := g_s \circ \dots \circ g_1(f_1(x^{(1)}), \dots, f_u(x^{(u)}), x^{(1)}, \dots, x^{(u)}),$$

where f_1, \dots, f_u are black-box functions, and g_1, \dots, g_s are known functions. As long as all the involved functions are continuous, we can model the black-box functions f_1, \dots, f_u with locally consistent SPs, and set a GNEB UQ $\hat{\sigma}(\tilde{x}; \mathcal{D}_n)$ as $\max(\hat{\sigma}(x^{(1)}; \mathcal{D}_n^{(1)}), \dots, \hat{\sigma}(x^{(u)}; \mathcal{D}_n^{(u)}))$ where $\mathcal{D}_n^{(i)}$ denotes the data collected by querying the black-box function f_i at the n -th iteration. With an AF satisfying the improvement property, the algorithm enjoys the consistency guarantee:

Corollary 5.1. *Suppose g 's and f 's are continuous, and $\mathcal{X}^{(i)}$ is compact, $\forall i$. Applying individual locally consistent SPs for black-box functions f_1, \dots, f_k , the SP $\hat{F} := g_s \circ \dots \circ g_1(\hat{f}_1(x^{(1)}; \mathcal{D}_n^{(1)}), \dots, \hat{f}_u(x^{(u)}; \mathcal{D}_n^{(u)}), x^{(1)}, \dots, x^{(u)})$ is locally consistent. Additionally, suppose $\hat{\sigma}(x^{(i)}; \mathcal{D}_n^{(i)})$ is GNEB for all i , then UQ $\hat{\sigma}(x^{(1)}, \dots, x^{(u)}; \mathcal{D}_n) := \max(\hat{\sigma}(x^{(1)}; \mathcal{D}_n^{(1)}), \dots, \hat{\sigma}(x^{(u)}; \mathcal{D}_n^{(u)}))$ is also GNEB. With an AF satisfying Assumption 3.5, the assembled PseudoBO algorithm is consistent.*

6. From Theory to Implementation

Our next goal is to leverage the PseudoBO recipe to construct empirically superior algorithms. We make the following considerations in choosing our ingredients for implementation:

Measuring UQ Quality. To look for a good UQ, we propose a criterion called *calibrated coverage rate (CCR)*, which considers the quality of both SP and UQ. Given a training set $\mathcal{D}_{\text{train}} := (X_{\text{train}}, Y_{\text{train}})$, a validation set $\mathcal{D}_{\text{val}} := (X_{\text{val}}, Y_{\text{val}})$, and a test set $\mathcal{D}_{\text{test}} := (X_{\text{test}}, Y_{\text{test}})$, suppose we have a pretrained SP $\hat{\mu}(\cdot; \mathcal{D}_{\text{train}})$ and UQ $\hat{\sigma}(\cdot; \mathcal{D}_{\text{train}})$. We compute the coverage rate of the prediction interval by

$$\mathbb{P}_{(x,y) \sim \mathcal{D}_{\text{test}}} (x \in [\hat{f}(x; \mathcal{D}_{\text{train}}) - \lambda_{\text{val}} \hat{\sigma}(x; \mathcal{D}_{\text{train}}), \hat{f}(x; \mathcal{D}_{\text{train}}) + \lambda_{\text{val}} \hat{\sigma}(x; \mathcal{D}_{\text{train}})]),$$

with $\lambda_{\text{val}} = \min_{\lambda \geq 0} \lambda$ such that $\mathbb{P}_{(x,y) \sim \mathcal{D}_{\text{val}}} (x \in [\hat{f}(x; \mathcal{D}_{\text{train}}) - \lambda \hat{\sigma}(x; \mathcal{D}_{\text{train}}), \hat{f}(x; \mathcal{D}_{\text{train}}) + \lambda \hat{\sigma}(x; \mathcal{D}_{\text{train}})]) = 1$. The higher the coverage is on the test set, the better the UQ is calibrated.

Model Configuration. We configure the following models: PseudoBO with SP and UQ as randomized prior's mean and standard deviation (PseudoBO-RP) with inner regressor as kernel regression, and PseudoBO with SP and UQ as kernel regression and a hybrid combination of minimum distance and randomized prior's standard deviation (PseudoBO-KR-Hyb), defined as:

$$\sigma_{\text{Hyb}}(x; \mathcal{D}_n) = \alpha_n \sigma_{\text{MD}}(x, \mathcal{D}_n) + (1 - \alpha_n) \sigma_{\text{RP}}(x, \tilde{\mathcal{D}}_n), \text{ with } \alpha_n := e^{-\Delta(x; \{x_n\})^n}, \quad (5)$$

where $\tilde{\mathcal{D}}_n$ denotes the bootstrapped data. The intuition of constructing this UQ is that randomized prior and bootstrapping together can best quantify the local uncertainty. However, randomized prior with bootstrapping is not guaranteed to have the GNEB property. The latter can be achieved via a hybrid version that combines with the minimum-distance UQ, where $\alpha_n \rightarrow 1$ as x gets closer to \mathcal{D}_n . Lastly, we also try the combination of Trust region and PseudoBO-KR-Hyb, shorthanded as

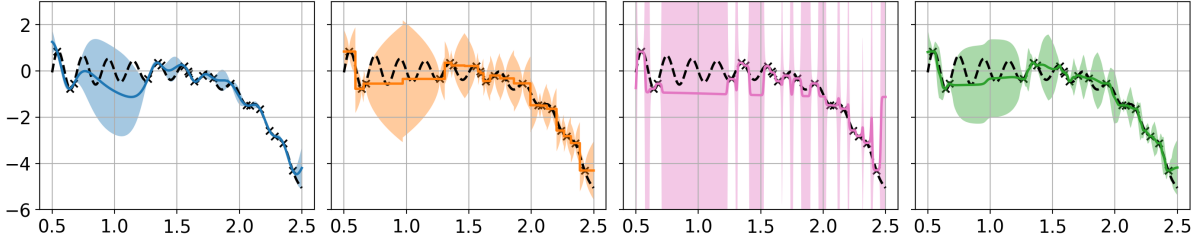


Fig. 2. A sample run of GP, NN+MD, RP, KR+Hybrid (from left to right). GP has CCR 0.85 and width 1.00, NN + MD has CCR 1.0 and width 1.89, RP has CCR 0.9 and width 12.73, and KR + Hybrid has CCR 0.98 and width 1.55.

PseudoBO-KR-Hyb-TR.

Optimizing EW. From our empirical investigation, we recommend using a scrambled Sobol sequence and pick the point with the largest EW among the sequence. This appears to enhance our performance compared with random search or BFGS.

7. Empirical Evaluations

In this section, we perform extensive empirical experiments on a wide range of tasks: a toy example for testing the quality of uncertainty quantification of surrogates, 4 synthetic black-box function optimizations, 4 hyperparameter tuning tasks, and 2 robotic tasks. All of these tasks are challenging and contain many local minima. The baseline models we consider in all the tasks comprise the standard BO, Random Search (RS) [8], SMAC, TPE, BORE, and LFBO. In particular, BO is implemented using BoTorch [4], and SMAC is implemented using AutoML [34]. In the large scale robotic experiments 7.4 and 7.5, we also include Turbo for comparison.

For acquisition function, BO, SMAC, and our PseudoBO variants use EI; TPE, BORE are designed to model PI; LFBO models EI; Turbo is designed optimally with Thompson sampling. Additional details regarding our experiments can be found in Appendix 15.

7.1. Calibration on the UQ

We start by comparing the quality of uncertainty quantification of different types of PseudoBO surrogate models: GP, NN + MD, RP, and KR + Hybrid by testing their CRRs. We test on three 1D benchmark functions: $f_1(x) = (\sin(\pi w))^2 + (w - 1)^2 \cdot (1 + \sin(2\pi w))^2$, where $w := 1 + (x - 1)/4$, $x \in [-10, 10]$; $f_2(x) = -20e^{-0.2|x|} - e^{\cos(2\pi x)} + 20 - e$, $x \in [-10, 5]$; $f_3(x) = \sin(10 \cdot \pi x)/(2x) + (x - 1)^4$, $x \in [0.5, 2.5]$. We generate the training set $\mathcal{D}_{\text{train}}$, the validation set \mathcal{D}_{val} and the test set $\mathcal{D}_{\text{test}}$ by uniformly sampling 20, 10 and 150 points from the search domain at random, with their labels evaluated by the benchmark function. The bisection method is used to find λ_{val} .

Methods	f_1		f_2		f_3	
	CCR	width	CCR	width	CCR	width
GP	0.91(± 0.12)	5.09(± 2.38)	0.93 (± 0.04)	6.29(± 1.15)	0.94(± 0.04)	1.57(± 0.19)
NN + MD	0.92(± 0.06)	5.37(± 1.90)	0.91(± 0.07)	4.11(± 0.93)	0.96 (± 0.03)	1.59(± 0.04)
RP	0.88(± 0.10)	62.29(± 43.96)	0.89(± 0.07)	76.48(± 27.02)	0.93(± 0.04)	20.46(± 8.47)
KR + Hybrid	0.93 (± 0.07)	5.34(± 1.63)	0.92(± 0.08)	4.45(± 1.05)	0.96 (± 0.04)	0.93(± 0.36)

Table 1. Coverage rate and UQ width of calibrated surrogates on the $\mathcal{D}_{\text{test}}$. Results are repeated for 10 runs.

From Table 1, we see that KR + Hybrid has the highest CCR in two out of the three test cases. GP and NN + MD have the highest CCR in one test case. RP achieves lower CCRs and large calibrated widths possibly because even if RP is designed for quantifying uncertainty for unexplored areas, without

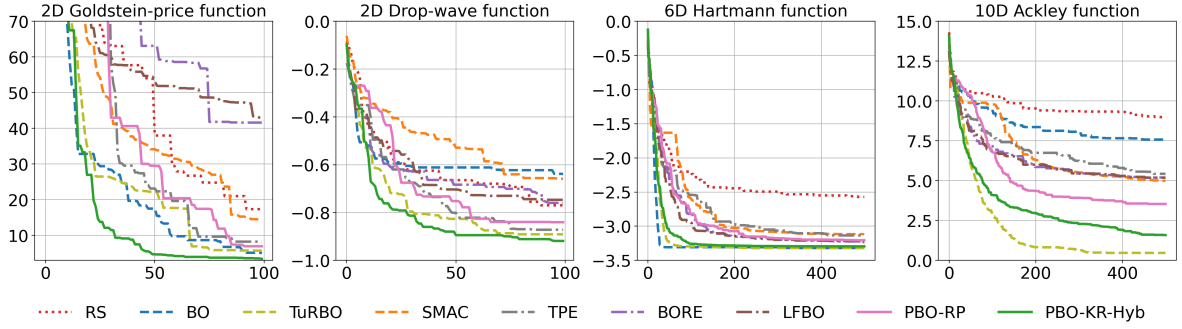


Fig. 3. Synthetic blackbox function minimization task. At each iteration t , the best objective queried is recorded. Each curve is an average over 10 runs.

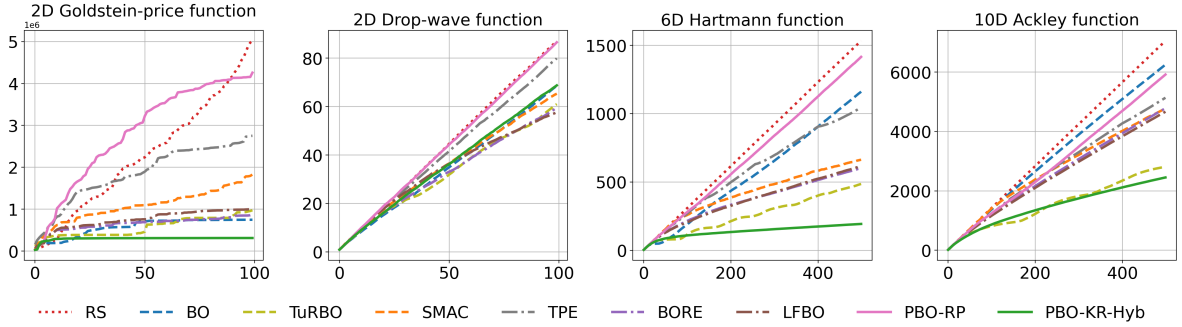


Fig. 4. Synthetic blackbox function minimization task. At each iteration t , the cumulative regret is recorded. Cumulative regret on synthetic blackbox function minimization task. Each curve is an average over 10 runs.

bootstrapping on the training set, its uncertainty quantification for local areas is less precise. To be concrete, Fig. 2 shows some exemplified results on three benchmarks.

7.2. Synthetic Black-Box Function Optimization

We perform testing in the minimization tasks of 4 well-known benchmark functions, including a 2D Goldstein-price function, a 2D Drop-wave function, a 6D Hartmann function, and a 10D Ackley function. For all the methods, we run 100 iterations with 5 initial samples for the two 2D functions, 500 iterations with 10 initial samples for the other two with higher dimensions. From Fig. 3, we see that PseudoBO-KR-Hyb achieves the lowest objective in three out of four tasks within the query budget. TuRBO demonstrates competitive performance by reaching the lowest objective in two out of four tasks. Moreover, we record the cumulative regret in Fig. 4. PseudoBO-KR-Hyb has sublinear cumulative regrets in time in all cases and is the best in three out of four tasks.

7.3. Hyperparameter Tuning

For a more realistic task, we test the methods applied to neural network tuning [30]. Our main goal here is to find the optimal set of hyperparameters for a two-layered fully connected neural network, to achieve the best training outcomes on four UCI datasets. There are 9 of them, including initial learning rate, learning rate schedule, batch size, and dropout rates, number of units, and activation function type for each of the two layers. This results in an expansive search space comprising 62,208 possible configurations in total. Fig. 5 reveals that among all the methods, PseudoBO-KR-Hyb is the fastest one to uncover the optimal configuration in three out of four tasks. PseudoBO-RP does not perform well here possibly because the randomized prior does not produce a good fit for the tree-structure function in this task. Relatively competitive models in this task are LFBO, BORE, and SMAC: LFBO achieves the best

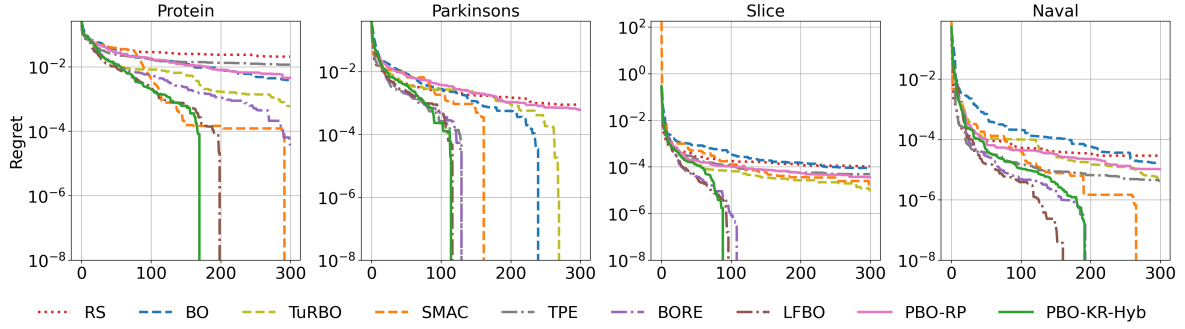


Fig. 5. Neural network tuning task. At each iteration t , the instant regret (defined as the current best validation loss subtracted by the validation loss of the optimal structure) is recorded. Each curve is an average over 25 runs.

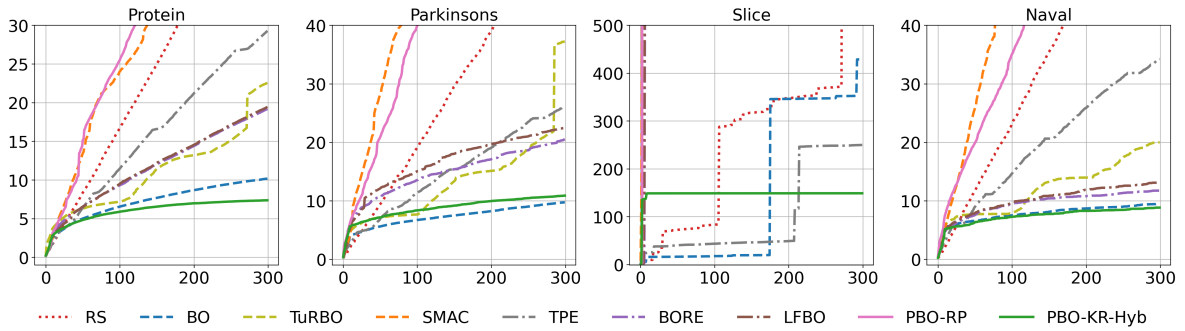


Fig. 6. Neural network tuning task. At each iteration t , the cumulative regret is recorded. Each curve is an average over 25 runs.

in the Naval task and quite close to PseudoBO-KR-Hyb in the Parkinsons task. BORE and SMAC find out the optimal configurations in three out of four tasks. Besides, we also record the cumulative regret for all methods in Fig. 6. The plot shows that PseudoBO-KR-Hyb has sublinear cumulative regret in time and has the lowest cumulative regret in three out of four tasks. In the second task, BO has the lowest cumulative regret. Although BO finds out the best configuration in only one dataset, its cumulative regrets in these tasks are competitive.

7.4. Robot Arm Pushing

This is a robotic problem to control the two robot arms with 14 parameters to push the two objects to the target positions. The reward is evaluated by the ending positions of the two objects pushed by two robot arms. See [62] for more details. In this task, we follow the procedure and setup in [18], conducting a batch of 50 queries in each iteration and performing optimization with a budget of 10000 queries. All methods are initialized with 100 queries. As demonstrated in Fig. 7 (1), all PseudoBO variants, particularly PseudoBO-KR-Hyb, converge significantly faster than other methods iteration-wise and eventually achieve a superior reward to most, except for TuRBO. When measured in runtime, Fig. 7 (2) illustrates that PseudoBO variants take merely 20s to achieve a reward of around 9 while most of the other methods remain at around 7, and TPE is around 8.5. It is also noteworthy that BO ceases at the 9,250-th query due to GPU being out of memory. A point to note is that Hyperopt (the package implementing TPE) doesn't support batch evaluation. Consequently, TPE queries and proposes the next point sequentially, allowing it to utilize more information than other methods. This means its performance might decline if batch evaluation were possible.

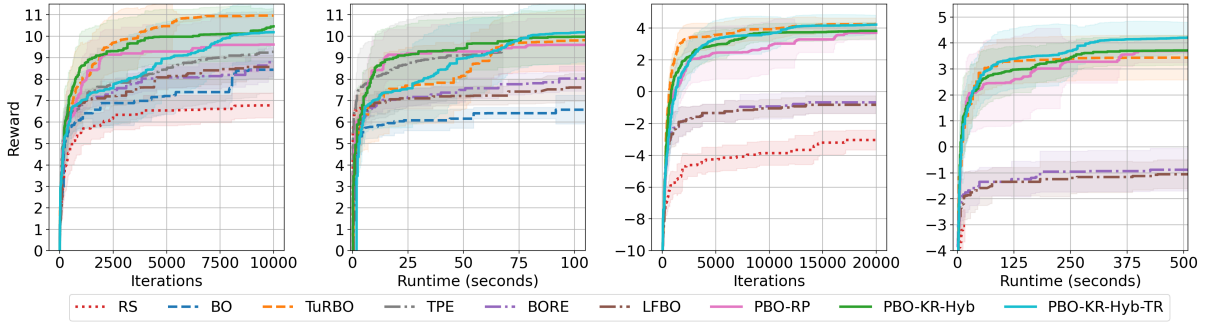


Fig. 7. Robot pushing task (first two) and Rover Trajectory task (last two). At each iteration n , the so far best reward is recorded. Each curve is an average over 10 runs. Shaded area is formed by \pm one standard deviation.

7.5. Rover Trajectory Planning

An additional robotic task is about rover trajectory optimization by determining the locations of 30 points in a 2D plane, where the final reward is estimated by the ending position of the rover and cost incurred by collision. See [62] for more details. We follow the procedure and setup in [18] to perform a batch of queries of size 100 in each iteration and execute optimization within a 20,000-query budget. All methods are started with 200 queries. Due to the memory issue, BO is not tested here. Besides, TPE is excluded from the test either, as sequentially querying and proposing took excessively long time to finish 20,000 queries. Fig. 7 (3) shows in terms of iterations, TuRBO converges slightly faster at the outset, but is later caught up by PseudoBO-KR-Hyb-TR. Besides, all PseudoBO variants converge more rapidly than other methods and ultimately secure considerably better final rewards. In terms of runtime, Fig. 7 (4) shows TuRBO converges as fast as PseudoBO-KR-Hyb-TR initially, but is surpassed by PseudoBO-KR-Hyb-TR at 125s, and later by PseudoBO-RP and PseudoBO-KR-Hyb at 400s. Eventually, PseudoBO-RP and PseudoBO-KR-Hyb yield rewards of around 3.8, PseudoBO-KR-Hyb-TR around 4.2 while TuRBO only reaches 3.5.

7.6. Runtime Record

We close our discussion by comparing the runtimes of the considered methods. Table 2 enumerates the runtimes of all tested methods to complete the target number of queries in various tasks. Some entries are vacant because the corresponding methods were not included in our experimental design. For smaller-scale experiments, we exclude PseudoBO-KR-Hyb-TR as scalability is not a concern; in the larger-scale tasks, BO is eliminated due to memory exhaustion, while SMAC and TPE are not included due to their packages' inability to support batch selection of candidates.

In small-sized tasks, our record reveals that RS and TPE demonstrate shorter runtimes than others. Immediately following these are the methods including BORE, LFBO, PseudoBO-RP, and PseudoBO-KR-Hyb, which all exhibit comparable runtimes. Despite being not as fast as the two methods above, their performances are usually more promising in comparison (especially in the neural network tuning task). While TuRBO is generally faster than BO, its runtime can be inconsistent. In the task of 10D synthetic function optimization, it considerably outpaces most of other methods, but this is not the case in the 12D NN Tuning task. This variability might arise from the restarting mechanism in the trust region method. Finally, both BO and SMAC consistently take the longest to complete the designated number of queries.

As the query budget grows up to tens of thousands in the robotic tasks, RS and TPE still stand as the fastest tier in terms of the runtime, immediately followed by the PseudoBO family. Notably, the scalability of the latter becomes even more apparent in these tasks in the sense that the time gap with TPE narrows and the PseudoBO family outperforms in terms of attained objective value significantly. Compared with other methods, in the 14D robotic task, the fastest PseudoBO model (PseudoBO-KR-

Hyb-TR) is 5X faster than BORE, 5X than LFBO, 4X than TuRBO and **60X** than BO. Likewise, in the 60D robotic task, PseudoBO-KR-Hyb-TR is 2.5X faster than BORE, 4X than LFBO and 5X than TuRBO. Fig. 8 shows a Pareto plot to illustrate the balancing effect of the optimal objective value attained eventually and runtime.

Tasks Queries	Synthetic (10D)	NN Tuning (12D)	Robot Push (14D)	Rover (60D)
	500	300	10,000	20,000
RS	1.00	2.00	5.37	16.73
BO	399.90*	791.40*	6202.55*	-
SMAC	747.4	200.14	-	-
TPE	16.50	6.00	67.78	-
BORE	37.10	17.20	514.37	1361.19
LFBO	66.70	23.88	575.38	2130.78
TuRBO	20.5*	56.08*	496.09*	2572.82*
PseudoBO-RP	42.03	32.90	127.55	513.08
PseudoBO-KR-Hyb	72.01	20.60	343.93	1453.00
PseudoBO-KR-Hyb-TR	-	-	107.22	510.60

Table 2. Runtime records in all types of tasks. Entries are in the unit of seconds. * on the top right of the entries means that the corresponding model was run on a GPU; otherwise, only CPU was used. Without GPU’s acceleration, even TuRBO (one of the most scalable state-of-the-art BO variants) takes approximately **4 hours** to complete one run for the 60D Rover task.

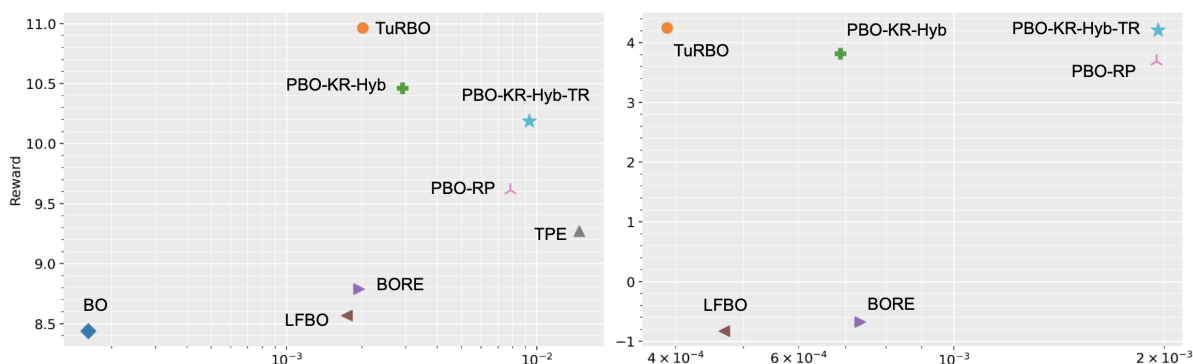


Fig. 8. Pareto plots of runtimes vs optimal objectives attained eventually in the reinforcement learning tasks (left for robot pushing and right for rover trajectory). In these visual representations, the effectiveness of a method increases alongside its position towards the upper right quadrant. The x-axis denotes the runtime with the transformation of $\log(\frac{1}{\text{runtime}})$ for the purpose of visualization.

Acknowledgements

We gratefully acknowledge support from the Amazon CAIT Fellowship, as well as the InnoHK initiative, the Government of the HKSAR, and Laboratory for AI-Powered Financial Technologies.

References

1. R. Astudillo and P. Frazier. Bayesian optimization of composite functions. In *International Conference on Machine Learning*, pages 354–363. PMLR, 2019.
2. R. Astudillo and P. Frazier. Bayesian optimization of function networks. *Advances in neural information processing systems*, 34:14463–14475, 2021.
3. Y. Bai, H. Lam, T. Balch, and S. Vyetrenko. Efficient calibration of multi-agent simulation models from output series with bayesian optimization. In *Proceedings of the Third ACM International Conference on AI in Finance*, pages 437–445, 2022.

4. M. Balandat, B. Karrer, D. R. Jiang, S. Daulton, B. Letham, A. G. Wilson, and E. Bakshy. BoTorch: A Framework for Efficient Monte-Carlo Bayesian Optimization. In *Advances in Neural Information Processing Systems* 33, 2020.
5. R. R. Barton, H. Lam, and E. Song. Input uncertainty in stochastic simulation. In *The Palgrave Handbook of Operations Research*, pages 573–620. Springer, 2022.
6. J. Bect, F. Bachoc, and D. Ginsbourger. A supermartingale approach to gaussian process based sequential design of experiments. *arXiv preprint arXiv:1608.01118*, 2016.
7. J. Bergstra, R. Bardenet, Y. Bengio, and B. Kégl. Algorithms for hyper-parameter optimization. *Advances in neural information processing systems*, 24, 2011.
8. J. Bergstra and Y. Bengio. Random search for hyper-parameter optimization. *Journal of machine learning research*, 13(2), 2012.
9. S. Bochner. *Harmonic analysis and the theory of probability*. Courier Corporation, 2005.
10. E. Brochu, V. M. Cora, and N. De Freitas. A tutorial on bayesian optimization of expensive cost functions, with application to active user modeling and hierarchical reinforcement learning. *arXiv preprint arXiv:1012.2599*, 2010.
11. A. D. Bull. Convergence rates of efficient global optimization algorithms. *Journal of Machine Learning Research*, 12(10), 2011.
12. R. Calandra, A. Seyfarth, J. Peters, and M. P. Deisenroth. Bayesian optimization for learning gaits under uncertainty: An experimental comparison on a dynamic bipedal walker. *Annals of Mathematics and Artificial Intelligence*, 76:5–23, 2016.
13. O. Chapelle and L. Li. An empirical evaluation of thompson sampling. *Advances in neural information processing systems*, 24, 2011.
14. C. Chevalier and D. Ginsbourger. Fast computation of the multi-points expected improvement with applications in batch selection. In *Learning and Intelligent Optimization: 7th International Conference, LION 7, Catania, Italy, January 7-11, 2013, Revised Selected Papers*, pages 59–69. Springer, 2013.
15. C. G. Corlu, A. Akcay, and W. Xie. Stochastic simulation under input uncertainty: A review. *Operations Research Perspectives*, 7:100162, 2020.
16. L. Csató and M. Opper. Sparse on-line gaussian processes. *Neural computation*, 14(3):641–668, 2002.
17. B. Efron. *The jackknife, the bootstrap and other resampling plans*. SIAM, 1982.
18. D. Eriksson, M. Pearce, J. Gardner, R. D. Turner, and M. Poloczek. Scalable global optimization via local bayesian optimization. *Advances in neural information processing systems*, 32, 2019.
19. P. I. Frazier. A tutorial on bayesian optimization. *arXiv preprint arXiv:1807.02811*, 2018.
20. J. Gardner, G. Pleiss, K. Q. Weinberger, D. Bindel, and A. G. Wilson. Gpytorch: Blackbox matrix-matrix gaussian process inference with gpu acceleration. *Advances in neural information processing systems*, 31, 2018.
21. X. Glorot and Y. Bengio. Understanding the difficulty of training deep feedforward neural networks. In *Proceedings of the thirteenth international conference on artificial intelligence and statistics*, pages 249–256. JMLR Workshop and Conference Proceedings, 2010.
22. J. González, Z. Dai, P. Hennig, and N. Lawrence. Batch bayesian optimization via local penalization. In *Artificial intelligence and statistics*, pages 648–657. PMLR, 2016.
23. L. Györfi, M. Köhler, A. Krzyżak, and H. Walk. *A distribution-free theory of nonparametric regression*, volume 1. Springer, 2002.
24. A. Hebbal, L. Brevault, M. Balesdent, E.-G. Talbi, and N. Melab. Bayesian optimization using deep gaussian processes with applications to aerospace system design. *Optimization and Engineering*, 22:321–361, 2021.
25. J. Hensman, N. Fusi, and N. D. Lawrence. Gaussian processes for big data. *arXiv preprint arXiv:1309.6835*, 2013.
26. F. Hutter, H. H. Hoos, and K. Leyton-Brown. Sequential model-based optimization for general algorithm configuration. In *International conference on learning and intelligent optimization*, pages 507–523. Springer, 2011.
27. D. R. Jones. A taxonomy of global optimization methods based on response surfaces. *Journal of global optimization*, 21:345–383, 2001.
28. D. R. Jones, M. Schonlau, and W. J. Welch. Efficient global optimization of expensive black-box functions. *Journal of Global optimization*, 13(4):455, 1998.
29. E. Kaufmann, N. Korda, and R. Munos. Thompson sampling: An asymptotically optimal finite-time analysis. In *Algorithmic Learning Theory: 23rd International Conference, ALT 2012, Lyon, France, October 29-31, 2012. Proceedings* 23, pages 199–213. Springer, 2012.

30. A. Klein and F. Hutter. Tabular benchmarks for joint architecture and hyperparameter optimization. *arXiv preprint arXiv:1905.04970*, 2019.
31. N. Lawrence, M. Seeger, and R. Herbrich. Fast sparse gaussian process methods: The informative vector machine. *Advances in neural information processing systems*, 15, 2002.
32. M. Lázaro-Gredilla, J. Quinero-Candela, C. E. Rasmussen, and A. R. Figueiras-Vidal. Sparse spectrum gaussian process regression. *The Journal of Machine Learning Research*, 11:1865–1881, 2010.
33. J. Li and I. O. Ryzhov. Convergence rates of epsilon-greedy global optimization under radial basis function interpolation. *Stochastic Systems*, 13(1):59–92, 2023.
34. M. Lindauer, K. Eggenberger, M. Feurer, A. Biedenkapp, D. Deng, C. Benjamins, T. Ruhkopf, R. Sass, and F. Hutter. Smac3: A versatile bayesian optimization package for hyperparameter optimization. *Journal of Machine Learning Research*, 23(54):1–9, 2022.
35. C. Liu and Y.-X. Wang. Global optimization with parametric function approximation. In *International Conference on Machine Learning*, pages 22113–22136. PMLR, 2023.
36. M. Locatelli. Bayesian algorithms for one-dimensional global optimization. *Journal of Global Optimization*, 10(1):57, 1997.
37. R. Marchant and F. Ramos. Bayesian optimisation for intelligent environmental monitoring. In *2012 IEEE/RSJ international conference on intelligent robots and systems*, pages 2242–2249. IEEE, 2012.
38. R. Martínez-Cantín, N. de Freitas, A. Doucet, and J. A. Castellanos. Active policy learning for robot planning and exploration under uncertainty. In *Robotics: Science and systems*, volume 3, pages 321–328, 2007.
39. M. McIntire, D. Ratner, and S. Ermon. Sparse gaussian processes for bayesian optimization. In *UAI*, 2016.
40. A. Nayebi, A. Munteanu, and M. Poloczek. A framework for bayesian optimization in embedded subspaces. In *International Conference on Machine Learning*, pages 4752–4761. PMLR, 2019.
41. C. Oh, E. Gavves, and M. Welling. Bock: Bayesian optimization with cylindrical kernels. In *International Conference on Machine Learning*, pages 3868–3877. PMLR, 2018.
42. I. Osband, J. Aslanides, and A. Cassirer. Randomized prior functions for deep reinforcement learning. *Advances in Neural Information Processing Systems*, 31, 2018.
43. M. A. Osborne, R. Garnett, and S. J. Roberts. Gaussian processes for global optimization. In *3rd international conference on learning and intelligent optimization (LION3)*, pages 1–15. Springer-Verlag Berlin, Germany, 2009.
44. M. A. L. Pearce, M. Poloczek, and J. Branke. Bayesian optimization allowing for common random numbers. *Operations Research*, 70(6):3457–3472, 2022.
45. V. Perrone, R. Jenatton, M. W. Seeger, and C. Archambeau. Scalable hyperparameter transfer learning. *Advances in neural information processing systems*, 31, 2018.
46. D. Russo and B. Van Roy. Learning to optimize via posterior sampling. *Mathematics of Operations Research*, 39(4):1221–1243, 2014.
47. M. W. Seeger, C. K. Williams, and N. D. Lawrence. Fast forward selection to speed up sparse gaussian process regression. In *International Workshop on Artificial Intelligence and Statistics*, pages 254–261. PMLR, 2003.
48. D. Sha, K. Ozbay, and Y. Ding. Applying bayesian optimization for calibration of transportation simulation models. *Transportation Research Record*, 2674(10):215–228, 2020.
49. A. Shah and Z. Ghahramani. Parallel predictive entropy search for batch global optimization of expensive objective functions. *Advances in neural information processing systems*, 28, 2015.
50. B. Shahriari, K. Swersky, Z. Wang, R. P. Adams, and N. De Freitas. Taking the human out of the loop: A review of bayesian optimization. *Proceedings of the IEEE*, 104(1):148–175, 2015.
51. E. Snelson and Z. Ghahramani. Sparse gaussian processes using pseudo-inputs. *Advances in neural information processing systems*, 18, 2005.
52. J. Snoek, O. Rippel, K. Swersky, R. Kiros, N. Satish, N. Sundaram, M. Patwary, M. Prabhat, and R. Adams. Scalable bayesian optimization using deep neural networks. In *International conference on machine learning*, pages 2171–2180. PMLR, 2015.
53. J. Song, L. Yu, W. Neiswanger, and S. Ermon. A general recipe for likelihood-free bayesian optimization. In *International Conference on Machine Learning*, pages 20384–20404. PMLR, 2022.
54. J. T. Springenberg, A. Klein, S. Falkner, and F. Hutter. Bayesian optimization with robust bayesian neural networks. *Advances in neural information processing systems*, 29, 2016.
55. N. Srinivas, A. Krause, S. M. Kakade, and M. Seeger. Gaussian process optimization in the bandit setting: No regret and experimental design. *arXiv preprint arXiv:0912.3995*, 2009.
56. W. R. Thompson. On the likelihood that one unknown probability exceeds another in view of the evidence

- of two samples. *Biometrika*, 25(3-4):285–294, 1933.
57. L. C. Tiao, A. Klein, M. W. Seeger, E. V. Bonilla, C. Archambeau, and F. Ramos. Bore: Bayesian optimization by density-ratio estimation. In *International Conference on Machine Learning*, pages 10289–10300. PMLR, 2021.
 58. S. Toscano-Palmerin and P. I. Frazier. Bayesian optimization with expensive integrands. *arXiv preprint arXiv:1803.08661*, 2018.
 59. J. Ungredda, M. Pearce, and J. Branke. Bayesian optimisation vs. input uncertainty reduction. *ACM Transactions on Modeling and Computer Simulation (TOMACS)*, 32(3):1–26, 2022.
 60. E. Vazquez and J. Bect. Convergence properties of the expected improvement algorithm with fixed mean and covariance functions. *Journal of Statistical Planning and inference*, 140(11):3088–3095, 2010.
 61. J. Wang, S. C. Clark, E. Liu, and P. I. Frazier. Parallel bayesian global optimization of expensive functions. *Operations Research*, 68(6):1850–1865, 2020.
 62. Z. Wang, C. Gehring, P. Kohli, and S. Jegelka. Batched large-scale bayesian optimization in high-dimensional spaces. In *International Conference on Artificial Intelligence and Statistics*, pages 745–754. PMLR, 2018.
 63. C. White, W. Neiswanger, and Y. Savani. Bananas: Bayesian optimization with neural architectures for neural architecture search. In *Proceedings of the AAAI Conference on Artificial Intelligence*, volume 35, pages 10293–10301, 2021.
 64. J. Wu and P. Frazier. The parallel knowledge gradient method for batch bayesian optimization. *Advances in neural information processing systems*, 29, 2016.
 65. J. Xie, P. I. Frazier, and S. E. Chick. Bayesian optimization via simulation with pairwise sampling and correlated prior beliefs. *Operations Research*, 64(2):542–559, 2016.

Appendix

8. Methodological Definitions

8.1. SP

In addition to the SPs defined in the main body (kernel regression and the mean of randomized prior), the rest of the SPs that we have mentioned are described in more detail in this section.

8.1.1. GP's posterior mean as SP

Given the data X_n and their evaluations $f(X_n)$, GP assumes f follows a Gaussian process with a mean function $\mu_0(\cdot)$ and a covariance function \mathcal{K} . Its posterior mean based on $\{x_i, f(x_i)\}_{i=1}^n$ is

$$\hat{f}_{GP,n}(x_0) = \mathcal{K}(x_0, X_n) \mathcal{K}(X_n, X_n)^{-1} (f(X_n) - \mu_0(X_n)) + \mu_0(x_0) \quad (6)$$

8.1.2. Nearest neighbour predictor as SP

Given the data X_n and their evaluations $f(X_n)$, a nearest neighbour predictor evaluated at point x_0 is defined as:

$$\hat{f}_{NN,n}(x_0) = f(\arg \min_{x \in X_n} \|x - x_0\|) \quad (7)$$

8.1.3. Neural network as SP

Given the data X_n and their evaluations $f(X_n)$, a neural network predictor evaluated at point x_0 is defined as:

$$\hat{f}_{Net,n}(x_0; \theta^*) = f_{\sigma_N, \theta_N^*} \circ f_{\sigma_{N-1}, \theta_{N-1}^*} \circ \dots \circ f_{\sigma_1, \theta_1^*}(x_0), \quad (8)$$

where $f_{\sigma_i, \theta_i^*}(x') := \sigma_i(\theta_i^{*T} [x', 1])$, N denotes the number of layers, σ_i denotes any activation function, and $\theta^* := \arg \min_{\theta} \frac{1}{n} \sum_{k=1}^n (\hat{f}_{Net,n}(x_k; \theta) - f(x_k))^2$.

8.1.4. Regression tree as SP

Given the data X_n and their evaluations $f(X_n)$, a regression tree predictor evaluated at point x_0 is defined as $\hat{f}_{T^*,n}(x_0)$, where T^* the set of leaves obtained from

$$\min_T \sum_{k=1}^{|T|} \sum_{x_i \in R_k} (f(x_i) - \overline{f(P_k)})^2, \quad (9)$$

where $P_k := X_n \cap T_k$, and $\overline{f(P_k)}$ denotes the average of all labels within the region of the leaf P_k .

8.2. UQ

We also define the rest of the UQs below.

8.2.1. GP's posterior variance as UQ

Given the data X_n and their evaluations $f(X_n)$, GP assumes f follows a Gaussian process with a mean function $\mu_0(\cdot)$ and a covariance function \mathcal{K} . Its posterior variance based on $\{x_i, f(x_i)\}_{i=1}^n$ is

$$\hat{\sigma}_{GP,n}^2(x_0) = \mathcal{K}(x_0, x_0) - \mathcal{K}(x_0, X_n) \mathcal{K}(X_n, X_n)^{-1} \mathcal{K}(X_n, x_0). \quad (10)$$

Note that GP's posterior variance does not depend on the labels in our data.

8.2.2. Minimum distance as UQ

Given the data X_n and their evaluations $f(X_n)$, the minimum-distance UQ is defined as:

$$\hat{\sigma}_{MD,n}(x_0) = \hat{\sigma}(f(X_n)) \Delta(x_0, X_n),$$

where $\hat{\sigma}(f(X_n))$ denotes the standard deviation of $f(X_n)$.

9. Consistency of Evaluation Worthiness

Proof of Theorem 3.2:

Proof. Denote $\{x_n\}$ as the sequence of evaluation points chosen by PseudoBO, and correspondingly $\mathcal{D}_n = \{(x_1, f(x_1)), \dots, (x_n, f(x_n))\}$ is the data collection up to step n . Since \mathcal{X} is compact, $\{x_n\}$ has a convergent subsequence, say $\{x_{\pi(n)}\}$. By Assumption 3.1 part 2, we have $W_n(x_{\pi(n)}; \mathcal{D}_{\pi(n)-1}) \rightarrow 0$ and hence $\liminf_{n \rightarrow \infty} W_n(x_n; \mathcal{D}_{n-1}) = 0$. On the other hand, suppose there is a point, say $x' \in \mathcal{X}$, that is non-adherent to $\{x_n\}$, i.e., there is no subsequence in $\{x_n\}$ that converges to x' . Then, by Assumption 3.1 part 1, we have $\liminf_{n \rightarrow \infty} W_n(x'; \mathcal{D}_n) > 0$. But this is impossible because PseudoBO requires at each step $x_{n+1} \in \operatorname{argmax}_{x \in \mathcal{X}} W_n(x; \mathcal{D}_n)$, hence a contradiction.

The second conclusion of the theorem follows by a straightforward use of the continuity of f . More precisely, as \mathcal{X} is compact and f is continuous, $x^* \in \operatorname{argmax}_{x \in \mathcal{X}} f(x)$ is well-defined and there is a subsequence of $\{x_n\}$, say $\{x_{\pi'(n)}\}$, converging to x^* by our first conclusion above. Then we have $f(x_{\pi'(n)}) \rightarrow f(x^*) = Z^*$ by the continuity of f . This gives

$$Z^* \geq f(\hat{x}_n^*) \geq f(x_{\pi'(n)}) \rightarrow f(x^*) = Z^*,$$

which concludes $f(\hat{x}_n^*) \rightarrow Z^*$. □

10. Consistency of the More Specialized Framework

10.1. Translating GNEB of UQ to GNEB of EW

Proof of Theorem 3.6:

Proof. Consider a sequence $x_n \in \mathcal{X}$, and $A_n = E_f(S_n)$ for an arbitrary set sequence $S_n \subset \mathcal{X}$. Suppose $\Delta(x, S_n \cup \{x_n\}) > 0 \forall n$. Then, by Assumption 3.4 part 1, we have $\liminf_{n \rightarrow \infty} \hat{\sigma}(x; A_n \cup \mathcal{D}_n) > 0$. By Assumption 3.5 part 2, we must have $\liminf_{n \rightarrow \infty} W_n(x; A_n \cup \mathcal{D}_n) > 0$.

To verify Assumption 3.1 part 2, consider a sequence $x_n \in X$ that converges to x' , and $A_n = E_f(S_n)$ for an arbitrary set sequence $S_n \subset X$. By Assumption 3.4 part 2, we have $\hat{\sigma}(x_n; A_{n-1} \cup \mathcal{D}_{n-1}) \rightarrow 0$ where $\mathcal{D}_{n-1} = \{(x_1, f(x_1)), \dots, (x_{n-1}, f(x_{n-1}))\}$. Moreover, by Assumption 3.3 we have $\hat{f}(x_n; A_{n-1} \cup \mathcal{D}_{n-1}) \rightarrow f(x')$. Thus,

$$\zeta(\hat{f}(x_n; A_{n-1} \cup \mathcal{D}_{n-1}) - \max \Pi_f(A_{n-1} \cup \mathcal{D}_{n-1})) \leq \zeta(\hat{f}(x_n; A_{n-1} \cup \mathcal{D}_{n-1}) - f(x_{n-1})) \rightarrow \zeta(0) \leq 0,$$

by the assumed continuity of f and ζ , the increasing property of ζ and $\zeta(0) \leq 0$. Thus, by Assumption 3.5 part 1, we further have

$$W_n(x_n; A_{n-1} \cup \mathcal{D}_{n-1}) = g_n(\zeta(\hat{f}(x_n; A_{n-1} \cup \mathcal{D}_{n-1}) - \max \Pi_f(A_{n-1} \cup \mathcal{D}_{n-1})), \hat{\sigma}(x_n; A_{n-1} \cup \mathcal{D}_{n-1})) \rightarrow 0.$$

This concludes Assumption 3.1 part 2. □

11. Verifying Local Consistency

11.1. Posterior Mean of GP

Proof of Proposition 4.1:

Proof. Proposition 10 in [60] assumes that $f \in \mathcal{H}$, where \mathcal{H} denotes the RKHS of a centered GP. For any two sequences $\{x_n\}, \{y_n\} \subset \mathcal{X}$ that is compact, suppose $y_n \rightarrow y'$ such that y' is adherent to $\{x_n\}$, then the posterior mean of GP $\hat{f}(y_n; \mathcal{D}_n) \rightarrow f(y')$. To further show it satisfying our local consistency assumption, consider a sequence $\{x_n\} \subset \mathcal{X}$ that converges to x' , and $A_n = E_f(S_n)$ for an arbitrary set sequence $S_n \subset \mathcal{X}$. By definition, x' is an adherent point of $S_n \cup X_n$. Therefore, we have $\hat{f}(x_n; A_{n-1} \cup \mathcal{D}_{n-1}) \rightarrow f(x')$. □

11.2. Nearest-Neighbour

Proof of Proposition 4.2:

Proof. To show local consistency of Nearest-Neighbour predictor \hat{f} , suppose $\{x_n\}$ converges to x' , and $A_n = E_f(S_n)$ for an arbitrary set sequence $S_n \subset \mathcal{X}$. By definition, x' is an adherent point of $A_n \cup \mathcal{D}_n$. Define $x'_n := \arg \min_{y \in S_{n-1} \cup \{x_{n-1}\}} \|x_n - y\|$. We have $\hat{f}(x_n; A_{n-1} \cup \mathcal{D}_{n-1}) = f(x'_n)$. By the continuity of f , $\lim_{n \rightarrow \infty} \hat{f}(x_n; A_{n-1} \cup \mathcal{D}_{n-1}) = \lim_{n \rightarrow \infty} f(x'_n) = f(\lim_{n \rightarrow \infty} x'_n) = f(x')$, where the last but one equality is due to the continuity of f , and the last inequality follows by the fact that $x_n \rightarrow x'$. \square

11.3. Over-Parameterized Neural Network

Proof of Proposition 4.3:

Proof. To show local consistency of an over-parameterized neural network mean predictor \hat{f} that can fit perfectly on the collected data, suppose $\{x_n\}$ converges to x' , and $A_n = E_f(S_n)$ for an arbitrary set sequence $S_n \subset \mathcal{X}$. For a trivial case, if $x' \in A_n \forall n$, then we will have $\hat{f}(x_n; A_{n-1} \cup \mathcal{D}_{n-1}) = f(x')$, as x_n approaches x' . Otherwise, Define $u(t; x, y) : [0, 1] \rightarrow \mathbb{R}$ as $u(t; x, y) = \hat{f}(tx + (1-t)y)$. With our assumption that \hat{f} is defined and differentiable in \mathcal{X} , it follows by mean value theorem that there exists a $t' \in [0, 1]$ such that $u(1; x, y) = u(0; x, y) + u'(t'; x, y)$, i.e.,

$$\hat{f}(x_n; A_{n-1} \cup \mathcal{D}_{n-1}) = \hat{f}(x_{n-1}; A_{n-1} \cup \mathcal{D}_{n-1}) + \nabla \hat{f}(x'_n; A_{n-1} \cup \mathcal{D}_{n-1})^T (x_n - x_{n-1}),$$

where $x'_n := t'x_n + (1-t)x_{n-1}$. By Cauchy-Schwarz inequality,

$$\hat{f}(x_n; A_{n-1} \cup \mathcal{D}_{n-1}) \leq \hat{f}(x_{n-1}; A_{n-1} \cup \mathcal{D}_{n-1}) + \|\nabla \hat{f}(x'_n; A_{n-1} \cup \mathcal{D}_{n-1})\| \|x_n - x_{n-1}\|.$$

Since \hat{f} is L -lipschitz, we have

$$|\hat{f}(x_n; A_{n-1} \cup \mathcal{D}_{n-1}) - \hat{f}(x_{n-1}; A_{n-1} \cup \mathcal{D}_{n-1})| \leq L \cdot \|x_n - x_{n-1}\| = o(1) \quad (11)$$

by the convergence of $\{x_n\}$. According to the continuity of $|\cdot|$ and f , we have

$$\begin{aligned} & \lim_{n \rightarrow \infty} |\hat{f}(x_n; A_{n-1} \cup \mathcal{D}_{n-1}) - \hat{f}(x_{n-1}; A_{n-1} \cup \mathcal{D}_{n-1})| \\ &= \lim_{n \rightarrow \infty} |\hat{f}(x_n; A_{n-1} \cup \mathcal{D}_{n-1}) - f(x_{n-1})| \\ &= |\lim_{n \rightarrow \infty} \hat{f}(x_n; A_{n-1} \cup \mathcal{D}_{n-1}) - \lim_{n \rightarrow \infty} f(x_{n-1})| \\ &= |\lim_{n \rightarrow \infty} \hat{f}(x_n; A_{n-1} \cup \mathcal{D}_{n-1}) - f(x')| = 0, \end{aligned}$$

following Eqn. 11, and the first equality is due to our assumption on perfect fitting. Therefore, $\lim_{n \rightarrow \infty} \hat{f}(x_n; A_{n-1} \cup \mathcal{D}_{n-1}) = f(x')$. \square

11.4. Regression Tree

Proof of Proposition 4.4:

To prove the consistency of the regression tree model, we require additional assumptions on the continuity of f , splitting mechanism of the tree model, number of samples lying in each leaf:

- (1) f is Lipschitz
- (2) The number of samples contained in each leaf is in $o(n)$.
- (3) When splitting a node into leaves, each dimension $m \in [d]$, there is a positive probability that it can be chosen.
- (4) When splitting a node into leaves, at least η proportion of samples need to be contained by each of the new leaves, and $\eta \in (0, \frac{1}{2}]$.

Proof. Suppose $\{x_n\}$ converges to x' , and $A_n = E_f(S_n)$ for an arbitrary set sequence $S_n \subset \mathcal{X}$. Let us denote the room that x is contained in a tree T by $R_x^T \subset \mathbb{R}^d$, and thus $P_x = R_x^T \cap (S_n \cup X_n)$. Recall the prediction a regression tree as SP is $\hat{f}_{T,n-1}(x_n) = \sum_{x \in S_{n-1} \cup X_{n-1}} w(x) f(x)$, where $w(x) = \frac{1}{|P_x|}$ if $x \in R_x^T$; otherwise 0. Therefore, we will have

$$\hat{f}_{T,n-1}(x_n) - f(x') = \sum_{x \in S_{n-1} \cup X_{n-1}} w(x) (f(x) - f(x')) \lesssim \sum_{x \in S_{n-1} \cup X_{n-1}} w(x) \|x - x'\|,$$

by (1). Moreover, since $\|x - x'\| \leq \|x - x_n\| + \|x_n - x'\|$ and $x_n \rightarrow x'$, by triangular inequality, the above upper bound is equivalent to $\sum_{x \in S_{n-1} \cup X_{n-1}} w(x) \|x - x_n\|$. Therefore, if we can show $n \rightarrow \infty$, we will have $|P_{x_n}|$ shrink to 0, so we finish the proof.

For any $x \in \mathcal{X}$, denote the number of nodes passed by the tree with input x as $N(x, T)$. For all the leaves, the number of samples inside them is lower bounded $n\eta^{\min_{x \in \mathcal{X}} N(x, T)}$. Also, by our assumption (2), we must have $n\eta^{\min_{x \in \mathcal{X}} N(x, T)} = o(n)$, implying $\eta^{\min_{x \in \mathcal{X}} N(x, T)} = o(1)$ and $\min_{x \in \mathcal{X}} N(x, T) \rightarrow \infty$ as $n \rightarrow \infty$.

Therefore, for any $x \in \mathcal{X}$, by (3), there must exist a sequence r_n such that $r_n \rightarrow \infty$, and $\mathbb{P}(N(x, m, T) > r_n) \rightarrow 1 \forall m \in [d]$, as $n \rightarrow \infty$, where $N(x, m, T)$ denotes the number of nodes queried by x and split in dimension m . That means each dimension will be split infinitely many times in probability. Moreover, by (4), we must have $|P_x| = o_p(1)$. Therefore, we have $\hat{f}_{T,n-1}(x_n) \rightarrow f(x')$ in probability. \square

11.5. Kernel Regression

Proof of Proposition 4.5:

Proof. Denote $\sum_{j \leq n} K_{h_n}(x, x_j) + n^{-2} \cdot \mathbb{1}\{\sum_{j \leq n} K_{h_n}(x, x_j) = 0\}$ by C_n . Suppose x_n converges to x' , and $A_n = E_f(S_n)$ for an arbitrary set sequence $S_n \subset \mathcal{X}$. We pick $h_n = o(1)$ and $\liminf_{n \rightarrow \infty} h_{n-1}/\Delta(x_n, S_{n-1} \cup X_{n-1}) \geq 1$. Define $\Pi_n(S_{n-1} \cup X_{n-1}) := \{x \in S_{n-1} \cup X_{n-1} : \|x_n - x\| \leq h_{n-1}\}$, and a subsequence $x_{k(n)}$ where $\Pi_{k(n)}(S_{k(n)-1} \cup X_{k(n)-1}) \neq \emptyset$. For each $n \geq 1$,

$$\begin{aligned} \hat{f}(x_{k(n)}; A_{k(n)-1} \cup \mathcal{D}_{k(n)-1}) &= \sum_{i \leq k(n)-1} \frac{K_{h_{k(n)-1}}(x_{k(n)}, x_i)}{C_n} f(x_i) \\ &= \sum_{\tilde{x} \in \Pi_{k(n)}(S_{k(n)-1} \cup X_{k(n)-1})} w(x_{k(n)}, \tilde{x}) f(\tilde{x}), \end{aligned}$$

where $\sum_{\tilde{x} \in \Pi_{k(n)}(S_{k(n)-1} \cup X_{k(n)-1})} w(x_{k(n)}, \tilde{x}) = 1$. Since $\Delta(x_n; S_{n-1} \cup X_{n-1}) \rightarrow 0$, f is continuous, and $h_n = o(1)$, it follows that $f(\tilde{x}) \rightarrow f(x)$, $\forall \tilde{x} \in \Pi_{k(n)}(S_{k(n)-1} \cup X_{k(n)-1})$. By the facts that $\Delta(x_n; S_{n-1} \cup X_{n-1}) \rightarrow 0$, as $n \rightarrow \infty$, and $\liminf_{n \rightarrow \infty} h_{n-1}/\Delta(x_n, S_{n-1} \cup X_{n-1}) \geq 1$, we must have $C_k > 0, \forall k \geq n$, and thus $\lim_{n \rightarrow \infty} \hat{f}(x_n; A_{n-1} \cup \mathcal{D}_{n-1}) = \lim_{n \rightarrow \infty} \hat{f}(x_{k(n)}; A_{k(n)-1} \cup \mathcal{D}_{k(n)-1}) = f(x)$. \square

11.6. Mean of Randomized Prior

Recall the mean of the randomized prior method:

$$\hat{f}(x; \mathcal{D}_n) = \mathbb{E}_{r \sim \mathcal{R}}[\hat{f}_r(x; \mathcal{D}_n)] = \mathbb{E}_{r \sim \mathcal{R}}[r(x) + \tilde{f}(x; \mathcal{D}'_n)],$$

where $\mathcal{D}'_n := \{(x_i, f(x_i) - r(x_i))\}$, and \tilde{f} is a locally consistent predictor.

Proof of Proposition 4.6:

Proof. Suppose $\{x_n\}$ converges to x' , and $A_n = E_f(S_n)$ for an arbitrary set sequence $S_n \subset \mathcal{X}$. For each $r \sim \mathcal{R}$, by the definition of locally consistent predictor and the continuity of r , we have

$$\begin{aligned} \lim_{n \rightarrow \infty} \hat{f}_r(x_n; A_{n-1} \cup \mathcal{D}_{n-1}) &= \lim_{n \rightarrow \infty} r(x_n) + \tilde{f}(x_n; A'_{n-1} \cup \mathcal{D}'_{n-1}) \\ &= \lim_{n \rightarrow \infty} r(x_n) + \lim_{n \rightarrow \infty} \tilde{f}(x_n; A'_{n-1} \cup \mathcal{D}'_{n-1}) \\ &= r(x') + f(x') - r(x') = f(x'). \end{aligned} \tag{12}$$

Therefore, since $\hat{f}_r(x_n; A_{n-1} \cup \mathcal{D}_{n-1}) \rightarrow f(x')$ almost surely, then

$$\hat{f}(x_n; A_{n-1} \cup \mathcal{D}_{n-1}) = \mathbb{E}_{r \sim \mathcal{R}}[r(x_n) + \tilde{f}(x_n; \tilde{A}_{n-1} \cup \tilde{\mathcal{D}}_{n-1})] \rightarrow f(x').$$

□

11.7. Hybrid Surrogate Predictor

Proof of Proposition 4.7:

Proof. Given a class of locally consistent SPs, suppose $\{x_n\}$ converges to x' , and $A_n = E_f(S_n)$ for an arbitrary set sequence $S_n \subset \mathcal{X}$. By definition, we have

$$\lim_{n \rightarrow \infty} \sum_{i=1}^{|\hat{\mathcal{F}}|} \alpha_i \hat{f}_i(x_n; A_{n-1} \cup \mathcal{D}_{n-1}) = \sum_{i=1}^{|\hat{\mathcal{F}}|} \alpha_i \lim_{n \rightarrow \infty} \hat{f}_i(x_n; A_{n-1} \cup \mathcal{D}_{n-1}) = \sum_{i=1}^{|\hat{\mathcal{F}}|} \alpha_i f(x) = f(x),$$

with the assumption that $\sum_{i=1}^{|\hat{\mathcal{F}}|} \alpha_i = 1$.

□

12. Verifying Generalized No-Empty-Ball Property

12.1. Posterior Variance of GP

Recall the NEB property of GP in [60]:

Assumption 12.1 (NEB property). *A Gaussian process has NEB property if, for all sequence $\{x_n\}$ in \mathcal{X} and all x' in \mathcal{X} , the following statements are equivalent:*

1. x' is an adherent point of $\{x_n\}$.
2. $\hat{\sigma}_{GP,n}^2(x'; \mathcal{D}_n) \rightarrow 0$ as $n \rightarrow \infty$.

Here $\hat{\sigma}_{GP,n}^2(x'; \mathcal{D}_n)$ denotes the posterior variance of the GP with n points collected.

Proof of Proposition 4.8:

Proof. Proposition 10 in [60] verifies the NEB property of GP, under the assumptions that \mathcal{X} is compact, GP is centered, the kernel function \mathcal{K} of the GP is continuous and stationary, and the spectral density \mathcal{S} of GP with property of \mathcal{S}^{-1} being at most polynomial growth. We show the GNEB property below based on this result.

Denote the GP as $\xi(\cdot)$. To show the second way of Assumption 3.4, suppose x_n converges to x' , and $A_n = E_f(S_n)$ for an arbitrary set sequence $S_n \subset \mathcal{X}$. We have

$$\begin{aligned} \hat{\sigma}_{GP,n-1}^2(x_n; A_{n-1} \cup \mathcal{D}_{n-1}) &\stackrel{(a)}{\leq} \hat{\sigma}_{GP,n-1}^2(x_n; \mathcal{D}_{n-1}) \\ &\stackrel{(b)}{=} \text{Var}[\xi(x_n) - \hat{\mu}_{GP,n-1}(x_n; \mathcal{D}_{n-1})] \\ &\stackrel{(c)}{\leq} \text{Var}[\xi(x_n) - \xi(x_{n-1})] \\ &\stackrel{(d)}{=} \mathcal{K}(x_n, x_n) - 2\mathcal{K}(x_n, x_{n-1}) + \mathcal{K}(x_{n-1}, x_{n-1}) \stackrel{(e)}{\rightarrow} 0, \end{aligned}$$

where we define $\hat{\mu}_{GP,n-1}$ as the posterior mean of the GP, and inequality (a) follows by the fact that with more points sampled, the uncertainty/entropy of the GP decreases; the equality (b) follows by the definition of variance; the inequality (c) follows by the fact the posterior mean of GP is the best linear predictor in $\mathcal{L}^2(\mathbb{R}^{\mathcal{X}}, \mathcal{A}, \mathbb{P})$, where \mathcal{A} is the product σ -algebra on $\mathbb{R}^{\mathcal{X}}$ and \mathbb{P} is the probability

measure defined on $(\mathbb{R}^{\mathcal{X}}, \mathcal{A})$; the inequality (d) follows by the alternative definition of variance; and the convergence of (e) follows by the continuity of \mathcal{K} and convergence of X_n .

To show the first way of Assumption 3.4, suppose $\inf_n \Delta(x; S_n \cup X_n) > 0$. Therefore, x cannot be an adherent point of $S_n \cup X_n$. The implication of Assumption 12.1 from 2 to 1 tells us $\hat{\sigma}_{GP,n}^2(x'; A_n \cup \mathcal{D}_n) \not\rightarrow 0$, and since $\hat{\sigma}_{GP,n}^2(x'; A_n \cup \mathcal{D}_n) \geq 0$ and is monotonically non-increasing on n , we must have $\liminf_{n \rightarrow \infty} \hat{\sigma}_{GP,n}^2(x'; A_n \cup \mathcal{D}_n) > 0$. \square

12.2. Minimum Distance

Proof of Proposition 4.9:

Proof. To show the first way, suppose $\inf_n \Delta(x; S_n \cup X_n) > 0$. Then $\liminf_{n \rightarrow \infty} \Delta(x; S_n \cup X_n) \geq \inf_n \Delta(x; S_n \cup X_n) > 0$.

To show the second way, fixing a $n \in \mathbb{N}$, we have

$$\Delta(x_n; S_{n-1} \cup X_{n-1}) \leq \|x_n - x_{n-1}\| := \varepsilon(n).$$

Since $x_n \rightarrow x'$, $0 \leq \lim_{n \rightarrow \infty} \Delta(x_n; S_{n-1} \cup X_{n-1}) \leq \lim_{n \rightarrow \infty} \varepsilon(n) = 0$, we conclude $\lim_{n \rightarrow \infty} \Delta(x_n; S_{n-1} \cup X_{n-1}) = 0$. \square

12.3. Variance of Randomized Prior

Proof of Proposition 4.10:

Proof. We start with the second way. Suppose $\{x_n\}$ converges to x' , and $A_n = E_f(S_n)$ for an arbitrary set sequence $S_n \subset \mathcal{X}$. By picking h_n with the rate same as in section 11.5, the kernel regressor is locally consistent. Therefore, we have

$$\begin{aligned} & |\hat{f}_r(x_n; A_{n-1} \cup \mathcal{D}_{n-1}) - \mathbb{E}_{r \sim \mathcal{R}} \hat{f}_r(x_n; A_{n-1} \cup \mathcal{D}_{n-1})| \\ & \leq |\hat{f}_r(x_n; A_{n-1} \cup \mathcal{D}_{n-1}) - f(x')| + |f(x') - \mathbb{E}_{r \sim \mathcal{R}} [\hat{f}_r(x_n; A_{n-1} \cup \mathcal{D}_{n-1})]| = o(1) \end{aligned}$$

The first inequality follows by the triangular inequality and the second equality follows by Eqn. 12 and the local consistency of the mean of randomized prior. Thus,

$$\text{Var}_{r \sim \mathcal{R}} [\hat{f}_r(x_n; A_{n-1} \cup \mathcal{D}_{n-1})] = \mathbb{E}_{r \sim \mathcal{R}} [\hat{f}_r(x_n; A_{n-1} \cup \mathcal{D}_{n-1}) - \mathbb{E}_{r \sim \mathcal{R}} \hat{f}_r(x_n; A_{n-1} \cup \mathcal{D}_{n-1})]^2 \rightarrow 0.$$

To show the first way, suppose $\inf_n \Delta(x; S_n \cup X_n) > 0$. Because of h_n 's rate of order $o(1)$ to satisfy local consistency, there must exist an iteration n' such that $\forall n \geq n'$, $C_n = 0$, and therefore $\text{Var}_{r \sim \mathcal{R}} [\hat{f}_r(x_n; A_{n-1} \cup \mathcal{D}_{n-1})] = \text{Var}_{r \sim \mathcal{R}} [r(x_n)] > 0$. \square

12.4. Hybrid UQ

Proof of Proposition 4.11:

Proof. Given a class of UQs $\hat{\Sigma} := \{\hat{\sigma}_1, \hat{\sigma}_2, \dots\}$ with the GNEB property, to show the first way, suppose $\inf_n \Delta(x; S_n \cup X_n) > 0$, and $A_n = E_f(S_n)$ for an arbitrary set sequence $S_n \subset \mathcal{X}$. For any convex combination of $\hat{\Sigma}$,

$$\liminf_{n \rightarrow \infty} \sum_{i=1}^{|\hat{\Sigma}|} \alpha_i \hat{\sigma}_i(x; A_{n-1} \cup \mathcal{D}_{n-1}) = \sum_{i=1}^{|\hat{\Sigma}|} \alpha_i \liminf_{n \rightarrow \infty} \hat{\sigma}_i(x; A_{n-1} \cup \mathcal{D}_{n-1}) > 0,$$

where the last inequality is because of the first way of GNEB and the existence of positiveness of α_i in convex combination.

To show the second way, suppose $\{x_n\}$ converges to x' , and $A_n = E_f(S_n)$ for an arbitrary set sequence $S_n \subset \mathcal{X}$. For any convex combination of $\hat{\Sigma}$,

$$\lim_{n \rightarrow \infty} \sum_{i=1}^{|\hat{\Sigma}|} \alpha_i \hat{\sigma}_i(x_n; A_{n-1} \cup \mathcal{D}_{n-1}) = \sum_{i=1}^{|\hat{\Sigma}|} \alpha_i \lim_{n \rightarrow \infty} \hat{\sigma}_i(x_n; A_{n-1} \cup \mathcal{D}_{n-1}) = 0.$$

\square

Note that a convex combination of UQ is not a minimal requirement to achieve GNEB. Obviously, all we need is just the multipliers $\alpha_i \geq 0 \forall i$ but $\exists i, \alpha_i > 0$. However, from a practical perspective, supposing we have a class of well calibrated UQs, then we prefer not to scale each UQ too excessively. Therefore, a convex combination of them is more appropriate.

13. Verifying Improvement Property

13.1. Probability of Improvement

Proof of Proposition 4.12:

Proof. We view $\text{PI}(x; \mathcal{D}_n)$ in terms of $p_n, \hat{\sigma}_n$:

$$g_n(p_n, \hat{\sigma}_n) = \begin{cases} \Phi((p_n - \tau)/\hat{\sigma}_n), & \text{if } \hat{\sigma}_n > 0, \\ \mathbb{1}\{(p_n - \tau) > 0\}, & \text{if } \hat{\sigma}_n = 0. \end{cases} \quad (13)$$

To show the first point of the improvement property, suppose $\limsup_{n \rightarrow \infty} p_n = c_1 \leq 0$ and $\lim_{n \rightarrow \infty} \hat{\sigma}_n = 0$. When n becomes large enough, $p_n - \tau \leq 0$ for $\tau > 0$. In the first condition, we have

$$\lim_{n \rightarrow \infty} g_n(p_n, \hat{\sigma}_n) = \lim_{n \rightarrow \infty} \Phi\left(\frac{p_n - \tau}{\hat{\sigma}_n}\right) = \Phi\left(\lim_{n \rightarrow \infty} \frac{p_n - \tau}{\hat{\sigma}_n}\right) = 0$$

In the second condition, $\lim_{n \rightarrow \infty} \mathbb{1}\{(p_n - \tau) > 0\} = 0$ since $p_n - \tau \leq 0$ for large enough n . Therefore, $\lim_{n \rightarrow \infty} g_n(p_n, \hat{\sigma}_n) = 0$.

To show the second point of the improvement property, suppose $\liminf_{n \rightarrow \infty} p_n > -\infty$ and $\liminf_{n \rightarrow \infty} \hat{\sigma}_n = c_3 > 0$. Since $\liminf_{n \rightarrow \infty} p_n > -\infty$ and $\Phi(v) > 0$ in $\{v : v < 0\}$, $\liminf_{n \rightarrow \infty} \Phi\left(\frac{p_n - \tau}{\hat{\sigma}_n}\right) > 0$. \square

13.2. Expected Improvement

Proof of Proposition 4.13:

Proof. We view $\text{EI}(x; \mathcal{D}_n)$ in terms of $p_n, \hat{\sigma}_n$:

$$g_n(p_n, \hat{\sigma}_n) = \begin{cases} \hat{\sigma}_n \phi\left(\frac{p_n - \tau}{\hat{\sigma}_n}\right) + (p_n - \tau) \Phi\left(\frac{p_n - \tau}{\hat{\sigma}_n}\right), & \text{if } \hat{\sigma}_n > 0, \\ \max\{p_n - \tau, 0\}, & \text{if } \hat{\sigma}_n = 0. \end{cases} \quad (14)$$

To show the first point of the improvement property, suppose $\limsup_{n \rightarrow \infty} p_n = c_1 \leq 0$ and $\lim_{n \rightarrow \infty} \hat{\sigma}_n = 0$. When n becomes large enough, $p_n - \tau \leq 0$. In the first condition, we have

$$\begin{aligned} \lim_{n \rightarrow \infty} g_n(p_n, \hat{\sigma}_n) &= \lim_{n \rightarrow \infty} \hat{\sigma}_n \phi\left(\frac{p_n - \tau}{\hat{\sigma}_n}\right) + \lim_{n \rightarrow \infty} (p_n - \tau) \Phi\left(\frac{p_n - \tau}{\hat{\sigma}_n}\right) \\ &= 0 \cdot \phi\left(\lim_{n \rightarrow \infty} \frac{p_n - \tau}{\hat{\sigma}_n}\right) + \lim_{n \rightarrow \infty} (p_n - \tau) \Phi\left(\lim_{n \rightarrow \infty} \frac{p_n - \tau}{\hat{\sigma}_n}\right) \quad (\text{continuity of } \phi \text{ and } \Phi) \\ &= 0 + c_1 \cdot 0 = 0 \end{aligned}$$

In the second condition, since $p_n - \tau \leq 0$ for large enough n , $\lim_{n \rightarrow \infty} \max(p_n - \tau, 0) = 0$. Therefore, $\lim_{n \rightarrow \infty} g_n(p_n, \hat{\sigma}_n) = 0$.

To show the second point of the improvement property, suppose $\liminf_{n \rightarrow \infty} p_n > -\infty$ and $\liminf_{n \rightarrow \infty} \hat{\sigma}_n = c_3 > 0$.

We show that $g(p_n, \hat{\sigma}_n)$ is positive as long as $\hat{\sigma}_n > 0$ and $p_n > -\infty$:

$$\begin{aligned} \frac{\partial g(p_n, \hat{\sigma}_n)}{\partial p_n} &= \frac{\partial \hat{\sigma}_n \phi\left(\frac{p_n - \tau}{\hat{\sigma}_n}\right) + p_n - \tau \Phi\left(\frac{p_n - \tau}{\hat{\sigma}_n}\right)}{\partial p_n} \\ &= -\hat{\sigma}_n \cdot \frac{p_n - \tau}{\hat{\sigma}_n^2} \phi\left(\frac{p_n - \tau}{\hat{\sigma}_n}\right) + \Phi\left(\frac{p_n - \tau}{\hat{\sigma}_n}\right) + \frac{p_n - \tau}{\hat{\sigma}_n} \phi\left(\frac{p_n - \tau}{\hat{\sigma}_n}\right) \\ &= \Phi\left(\frac{p_n - \tau}{\hat{\sigma}_n}\right) \geq 0. \end{aligned}$$

Therefore, when the improvement p_n is smaller, the acquisition $g(p_n, \hat{\sigma}_n)$ is smaller.

$$\inf_{p_n \in \mathbb{R}} g_n(p_n, \hat{\sigma}_n) = \lim_{p_n \rightarrow -\infty} g(p_n, \hat{\sigma}_n) = \lim_{p_n \rightarrow -\infty} \hat{\sigma}_n \phi\left(\frac{p_n - \tau}{\hat{\sigma}_n}\right) + (p_n - \tau) \cdot \Phi\left(\frac{p_n - \tau}{\hat{\sigma}_n}\right) = \lim_{p_n \rightarrow -\infty} (p_n - \tau) \cdot \Phi\left(\frac{p_n - \tau}{\hat{\sigma}_n}\right)$$

To compute this, we leverage L'Hôpital's rule:

$$\lim_{p_n \rightarrow -\infty} (p_n - \tau) \cdot \Phi\left(\frac{p_n - \tau}{\hat{\sigma}_n}\right) = \lim_{p_n \rightarrow -\infty} \frac{\Phi\left(\frac{p_n - \tau}{\hat{\sigma}_n}\right)}{1/(p_n - \tau)} = \lim_{p_n \rightarrow -\infty} \frac{\frac{1}{\hat{\sigma}_n} \phi\left(\frac{p_n - \tau}{\hat{\sigma}_n}\right)}{-1/(p_n - \tau)^2} = \lim_{p_n \rightarrow -\infty} -\frac{(p_n - \tau)^2}{\hat{\sigma}_n} \phi\left(\frac{p_n - \tau}{\hat{\sigma}_n}\right) = 0.$$

Therefore, for any $\hat{\sigma}_n > 0$, as long as $p_n \in \mathbb{R}$, we have $g_n(p_n - \tau, \hat{\sigma}_n) > 0$. It follows that for any sequence p_n with $\liminf_{n \rightarrow \infty} p_n > -\infty$, $\liminf_{n \rightarrow \infty} g_n(p_n, \hat{\sigma}_n) > 0$. \square

13.3. Upper Confidence Bound

Proof of Proposition 4.14:

Proof. We view UCB($x; \mathcal{D}_n$) in terms of $p_n, \hat{\sigma}_n$: $g_n(p_n, \hat{\sigma}_n) = \frac{p_n - \tau}{\beta_n} + \hat{\sigma}_n$.

To show the first point of the improvement property, suppose $\limsup_{n \rightarrow \infty} p_n = c_1 \leq 0$ and $\lim_{n \rightarrow \infty} \hat{\sigma}_n = 0$. We have $\lim_{n \rightarrow \infty} \frac{p_n - \tau}{\beta_n} = 0$ since $\beta_n \geq 0$ and is strictly increasing in n . Therefore, $\lim_{n \rightarrow \infty} \frac{p_n - \tau}{\beta_n} + \hat{\sigma}_n = 0$.

To show the second point of the improvement property, suppose $\liminf_{n \rightarrow \infty} p_n > -\infty$ and $\liminf_{n \rightarrow \infty} \hat{\sigma}_n = c_3 > 0$. We also have $\lim_{n \rightarrow \infty} \frac{p_n - \tau}{\beta_n} = 0$ since $\beta_n \geq 0$ and is strictly increasing in n . Therefore, $\liminf_{n \rightarrow \infty} \frac{p_n - \tau}{\beta_n} + \hat{\sigma}_n = \liminf_{n \rightarrow \infty} \hat{\sigma}_n > 0$. \square

13.4. Hybrid Acquisition

Proof of Proposition 4.15:

Proof. Given a class of AFs with the improvement property $\mathcal{G} := \{g_1, g_2, \dots\}$, and suppose $\sum_{i=1}^{|\mathcal{G}|} \alpha_i = 1$ and $\alpha_i \geq 0$, the hybrid AF $\sum_{i=1}^{|\mathcal{G}|} \alpha_i g_i$ satisfies the first property because continuity is preserved under summation. Also, suppose $p \leq 0$ and $q = 0$, and thus $g_i(p, q) = 0$, then $\sum_{i=1}^{|\mathcal{G}|} \alpha_i g_i = 0$, which shows our second point. Similarly, if $q > 0$, then $\sum_{i=1}^{|\mathcal{G}|} \alpha_i g_i > 0$ by the definition of convex combination. The third point is verified. \square

Similar to hybrid UQ, we note that a convex combination of \mathcal{G} is not a minimal requirement to retain improvement property and one can generalize the multipliers to $\alpha_i \geq 0 \forall i$ but $\exists i, \alpha_i > 0$. However, convex combination is without loss of generality because it can be obtained if we normalize the weights by dividing them by their sum.

14. Composite Optimization

Proof of Corollary 5.1:

Proof. We first show the locally consistency of \hat{F} in order to achieve consistency of the PseudoBO algorithm. By definition of locally consistency, suppose we have a convergent sequence $\tilde{x}_n := (x_n^{(1)}, \dots, x_n^{(u)}) \in \Pi_{i=1}^u \mathcal{X}^{(i)}$ to $\tilde{x}' := (x'^{(1)}, \dots, x'^{(u)})$, then we have $\hat{f}_1(x_n^{(1)}; \mathcal{D}_{n-1}^{(1)}) \rightarrow f_1(x'^{(1)})$, ..., $\hat{f}_u(x_n^{(u)}; \mathcal{D}_{n-1}^{(u)}) \rightarrow f_u(x'^{(u)})$. By the continuity of g_1, \dots, g_s , the convergence continues to hold, and thus $\hat{F}(x_n^{(1)}; \mathcal{D}_{n-1}) \rightarrow F(\tilde{x}')$.

To show the GNEB property, we start with the first way. Suppose $\inf_n \Delta(x^{(1)}, \dots, x^{(u)}; S_n \cup X_u) > 0$, where $S_n := \Pi_{i=1}^u S_n^{(i)}$ for $S_n^{(i)} \subset \mathcal{X}^{(i)}$ and $X_n := \Pi_{i=1}^u X_n^{(i)}$ with $X_n^{(i)} := \{x_1^{(i)}, \dots, x_n^{(i)}\}$. This implies $\inf_n \Delta(x_n^{(i)}; S_n^{(i)} \cup X_u^{(i)}) > 0, \forall i$. Therefore, $\liminf_{n \rightarrow \infty} \max(\hat{\sigma}(x_n^{(1)}; A_{n-1}^{(1)} \cup \mathcal{D}_{n-1}^{(1)}), \dots, \hat{\sigma}(x_n^{(u)}; A_{n-1}^{(u)} \cup \mathcal{D}_{n-1}^{(u)})) \geq \liminf_{n \rightarrow \infty} \hat{\sigma}(x_n^{(i)}; A_{n-1}^{(i)} \cup \mathcal{D}_{n-1}^{(i)}) > 0, \forall i$ by the first way of GNEB property satisfied by individual UQ. For the second way, suppose $(x_n^{(1)}, \dots, x_n^{(u)}) \rightarrow (x'^{(1)}, \dots, x'^{(u)})$. For any set $S_n^{(i)} \subset \mathcal{X}^{(i)}$, we have $\hat{\sigma}(x_n^{(i)}; A_{n-1}^{(i)} \cup \mathcal{D}_{n-1}^{(i)}) \rightarrow 0, \forall i$. Therefore, $\lim_{n \rightarrow \infty} \max(\hat{\sigma}(x^{(1)}; A_n^{(1)} \cup \mathcal{D}_n^{(1)}), \dots, \hat{\sigma}(x^{(u)}; A_n^{(u)} \cup \mathcal{D}_n^{(u)})) = 0$.

Combining with an AF satisfying Assumption 3.5, we obtain the consistency of PseudoBO by Corollary 3.7. \square

15. Experiment Details

15.1. Implementations

The methods we compare with are listed in Table 3.

Methods	Software library	URL
RS	Hyperopt	https://github.com/hyperopt/hyperopt
BO	BoTorch	https://botorch.org
TuRBO	-	https://github.com/uber-research/TuRBO
TPE	Hyperopt	https://github.com/hyperopt/hyperopt
BORE	Syne Tune	https://github.com/awsmlabs/syne-tune
LFBO	-	https://github.com/lfbo-ml/lfbo

Table 3. Packages information

In particular, for BO, we use Matérn Kernel with default hyperparameters’ values in BoTorch. For BORE and LFBO models, we use XGBoost as the classifier, with preset parameters in their original implementations, since LFBO/BORE with XGBoost has relatively good and stable performance across tasks and computationally much faster than other classifiers (random forest or neural network).

All experiments are conducted on a computer with a 4-core Intel(R) Xeon(R) CPU @ 2.30GHz and a Tesla T4 GPU.

15.1.1. Hyperparameters for PseudoBO Models

Random prior functions The random functions in all tasks are sampled from a 3-layered random neural network $r(x) = W_3 \text{Tanh}(W_2 \text{Tanh}(W_1 x + b_1) + b_2) + b_3$, with Glorot random initialization [21].

Kernel We use Gaussian kernel throughout all models and all tasks.

Bandwidths To determine the bandwidth of kernel regression in the PseudoBO models, we follow the implication from the local consistency that SP should correctly estimate objective values the queried points and the analysis of upper minimax rate of convergence for kernel regression [23] in the nonparametric statistic literature. Particularly, for any random vector $(X, Y) \in R^d \times R$ that has $\text{Var}(Y|X = x) \leq \sigma^2$ and $\mathbb{E}(Y|X = x)$ is Lipschitz on x , with domain \mathcal{X} compact, picking the bandwidth $h_n = \mathcal{O}(n^{-\frac{1}{2+d}})$ leads to the best rate of convergence. Additionally, to ensure kernel regression generalizes well for the unexplored area, we allow the bandwidth to be larger than the relatively explored area. Therefore, we define the bandwidth as follows:

$$h_n^{(l)} = h_0^{(l)} \cdot n^{-\frac{1}{2+d}}, \quad h_n^{(u)} = h_0^{(u)} \cdot n^{-\frac{1}{2+d}}$$

$$h_n(x) = (1 - e^{-\Delta(x, X_n) \cdot n}) \cdot (h_n^{(u)} - h_n^{(l)}) + h_n^{(l)},$$

where $h_0^{(u)} \geq h_0^{(l)} > 0$.

For the bandwidth in the randomized prior method, we adopt $h'_n = h'_0 \cdot n^{-\frac{1}{2+d}}$.

From our empirical investigation, choosing $h_0^{(l)}$, $h_0^{(u)}$ and h'_0 to be small helps the performance of the PseudoBO models. Typically, supposing $\mathcal{X} = [0, 1]^d$, choosing $h_0^{(l)} \in [0.075, 0.1]$, $h_0^{(u)} \in [0.2, 0.4]$, and $h'_0 = 0.005$ (in hybrid randomized prior UQ) would produce a relatively promising performance.

Specifically, PseudoBO-RP uses $h'_{0,i} = 0.075(\mathcal{X}_{i,1} - \mathcal{X}_{i,0})$ for synthetic functions optimization; $h'_0 = 0.1 \times [1/2, 1/2, 1/2, 1/2, 1/4, 1/3, 1/3, 1/6, 1/2, 1/2, 1/6, 1/6]$ for neural network tuning, where the denominators in the vector represents the number of candidates in each hyperparameter (see Sec. 15.3 for further details); $h'_{0,i} = 0.1(\mathcal{X}_{i,1} - \mathcal{X}_{i,0})$ for both RL tasks.

PseudoBO-KR-Hyb/PseudoBO-KR-Hyb-TR uses $h'_0 = 0.01 \times [1/2, 1/2, 1/2, 1/2, 1/4, /3, 1/3, 1/6, 1/2, 1/2, 1/6, 1/6]$ in neural network tuning, and $h'_{0,i} = 0.005(\mathcal{X}_{i,1} - \mathcal{X}_{i,0})$ in all other tasks for UQ. For SP, they use $h_{0,i}^{(l)} = 0.05(\mathcal{X}_{i,1} - \mathcal{X}_{i,0})$, $h_{0,i}^{(u)} = 0.2(\mathcal{X}_{i,1} - \mathcal{X}_{i,0})$ in synthetic functions optimization; $h_{0,i} = 0.2 \times [1/2, 1/2, 1/2, 1/2, 1/4, /3, 1/3, 1/6, 1/2, 1/2, 1/6, 1/6]$, $h_{0,u} = 0.8 \times [1/2, 1/2, 1/2, 1/2, 1/4, /3, 1/3, 1/6, 1/2, 1/2, 1/6, 1/6]$ in neural network tuning; $h_{0,i}^{(l)} = 0.1(\mathcal{X}_{i,1} - \mathcal{X}_{i,0})$, $h_{0,i}^{(u)} = 0.325(\mathcal{X}_{i,1} - \mathcal{X}_{i,0})$ in robot pushing; $h_{0,i}^{(l)} = 0.1(\mathcal{X}_{i,1} - \mathcal{X}_{i,0})$, $h_{0,i}^{(u)} = 0.375(\mathcal{X}_{i,1} - \mathcal{X}_{i,0})$ in rover trajectory planning.

Perturbation probability of Sobol sequence As in Turbo [18], we use Sobol sequence for inner optimization of all PseudoBO models, with perturbing probability of 1 in the 2D synthetic function tasks, 0.75 in the 6D synthetic function task, 0.5 in the 10D synthetic function task, 0.4 in the 12D neural network tuning task, 0.35 in the 14D robot push task, and 0.15 for the 60D rover trajectory task.

Robust UQ In the task of neural network hyperparameter tuning, we observe that the collected query data bears a large deviation, resulting in a bad estimate of uncertainty quantification. Therefore, we perform winsorization on the data to ensure UQ to work robustly. In particular, for all the data with objectives smaller than $q_3 - 5(q_3 - q_1)$, we replace them with $q_3 - 5(q_3 - q_1)$, where q_1 and q_3 represents the first and third quartile of the data.

15.2. Calibrated Coverage Rate

In this task, we employ our proposed CCR criterion to assess how well the uncertainty quantification of GP, NN+MD, RP, KR+Hyb is calibrated. We generate the training set $\mathcal{D}_{\text{train}}$, the validation set \mathcal{D}_{val} and the test set $\mathcal{D}_{\text{test}}$ by uniformly sampling 20, 10 and 150 points from the search domain at random, with their labels evaluated by the blackbox function.

We have purposefully designed the size of $\mathcal{D}_{\text{train}}$, \mathcal{D}_{val} , and $\mathcal{D}_{\text{test}}$. The size of the validation set is smaller than the size of training set so that the calibration over the validation set does not disclose excessive information about the unknown function's shape. Consequently, the quality of calibration depends on a combination of learnings from the training set and supplementary information from the validation set. Moreover, the size of test set is much larger than both for the purpose of a more accurate evaluation of the natural calibration performance of each uncertainty quantification method.

To find $\lambda_{\text{val}} = \min_{\lambda \geq 0} \lambda$ s.t.

$$\mathbb{P}_{(x,y) \sim \mathcal{D}_{\text{val}}}(x \in [\hat{f}(x; \mathcal{D}_{\text{train}}) - \lambda \hat{\sigma}(x; \mathcal{D}_{\text{train}}), \hat{f}(x; \mathcal{D}_{\text{train}}) + \lambda \hat{\sigma}(x; \mathcal{D}_{\text{train}})]) = 1,$$

we propose algorithm 1:

Additional sample runs on the objective f_1 and f_2 are shown in Figures 9 and 10.

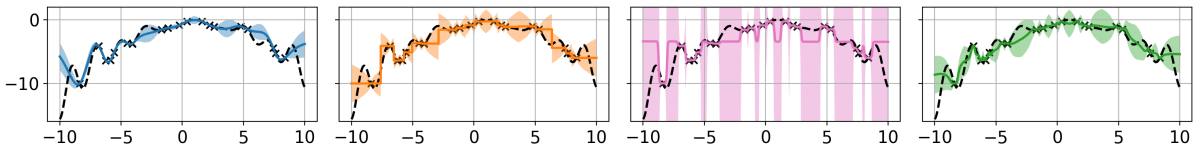


Fig. 9. A sample run of GP, NN+MD, RP, KR+Hybrid (from left to right). GP has CCR 0.57 and width 1.47, NN + MD has CCR 0.77 and width 3.06, RP has CCR 0.91 and width 71.50, and KR + Hybrid has CCR 0.86 and width 3.26.

Algorithm 1: Pre-trained SP and UQ Combo Calibration

Input: Pretrained SP $\hat{f}(\cdot; \mathcal{D}_{\text{train}})$, pretrained UQ $\hat{\sigma}(\cdot; \mathcal{D}_{\text{train}})$, validation set \mathcal{D}_{val} , and tolerance level ε ;
Output: Multiplier λ_{val} ;
Initialize $\lambda_l \leftarrow 0$, $\lambda_{\text{init}} \leftarrow 1$, $\lambda_u \leftarrow \infty$.
while $\lambda_u = \infty$ **do**
 Compute
 $CR_{\text{init}} \leftarrow \mathbb{P}_{(x,y) \sim \mathcal{D}_{\text{val}}}(x \in [\hat{f}(x; \mathcal{D}_{\text{train}}) - \lambda_{\text{init}} \hat{\sigma}(x; \mathcal{D}_{\text{train}}), \hat{f}(x; \mathcal{D}_{\text{train}}) + \lambda_{\text{init}} \hat{\sigma}(x; \mathcal{D}_{\text{train}})])$.
 if $CR_{\text{init}} < 1$ **then**
 | $\lambda_{\text{init}} \leftarrow 2 \cdot \lambda_{\text{init}}$.
 else
 | $\lambda_u \leftarrow \lambda_{\text{init}}$.
 end
end
while $\lambda_u - \lambda_l > \varepsilon$ **do**
 $\lambda_{\text{val}} \leftarrow (\lambda_l + \lambda_u) / 2$
 Compute
 $CR_{\text{val}} \leftarrow \mathbb{P}_{(x,y) \sim \mathcal{D}_{\text{val}}}(x \in [\hat{f}(x; \mathcal{D}_{\text{train}}) - \lambda_{\text{val}} \hat{\sigma}(x; \mathcal{D}_{\text{train}}), \hat{f}(x; \mathcal{D}_{\text{train}}) + \lambda_{\text{val}} \hat{\sigma}(x; \mathcal{D}_{\text{train}})])$.
 if $CR_{\text{val}} < 1$ **then**
 | $\lambda_l \leftarrow \lambda_{\text{val}}$.
 else
 | $\lambda_u \leftarrow \lambda_{\text{val}}$.
 end
end

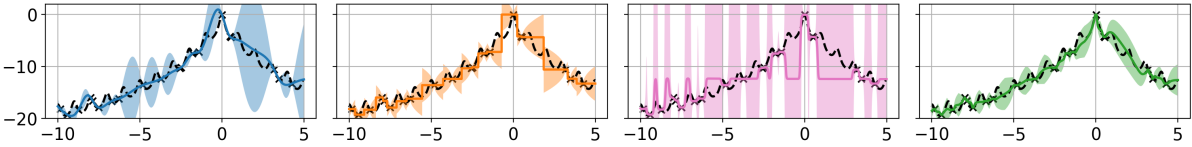


Fig. 10. A sample run of GP, NN+MD, RP, KR+Hybrid (from left to right). GP has CCR 0.86 and width 5.12, NN + MD has CCR 0.90 and width 3.63, RP has CCR 0.99 and width 126.53, and KR + Hybrid has CCR 0.93 and width 3.05.

15.3. Hyperparameter Tuning

This task originates from HPOBench [30]. The parameters to be tuned are shown in Table 4.

In this task, we follow the procedure in [57] to densify the search space by one-hot encoding for categorical hyperparameters (including LR Schedule, activation function of layers 1&2), with each variable with domain of $[0,1]$ representing each category. For each of other numerical hyperparameters, we use one variable with domain of $[0,1]$ with space equalized separated for all candidates of that hyperparameter. Therefore, the search domain is $[0, 1]^{12}$.

15.4. Robot Arm Pushing

This 14D task is designed for optimizing the controllers of the robot's two arms to push two objects to their target places o_1 and o_2 , starting from positions s_1 and s_2 . Let us denote the ending positions of the two objects by e_1 and e_2 , resulted from a specific control. The final reward is defined as

$$R(x) = \|s_1 - o_1\| + \|s_2 - o_2\| - (\|s_1 - e_1\| + \|s_1 - e_2\|).$$

Hyperparameter	Choices
Initial LR	{0.0005, 0.001, 0.005, 0.01, 0.05, 0.1}
Batch Size	{8, 16, 32, 64}
LR Schedule	{ cosine, fixed }
Activation of Layer 1	{ Tanh, ReLU }
Width of Layer 1	{16, 32, 64, 128, 256, 512}
Dropout rate of Layer 1	{0.0, 0.3, 0.6}
Activation of Layer 2	{ Tanh, ReLU }
Width of Layer 2	{16, 32, 64, 128, 256, 512}
Dropout rate of Layer 2	{0.0, 0.3, 0.6}

Table 4. Tunable hyperparameters and search space in the HBOBench task.

There are 14 parameters to control the location and rotation of the robot hands, pushing speed, moving direction and pushing time, presented in Table 5.

Hyperparameter of Arm 1/2	Ranges
Position x	$[-5, 5]$
Position y	$[-5, 5]$
Angle	$[0, 2\pi]$
Torque	$[-5, 5]$
Velocity v_x	$[-10, 10]$
Velocity v_y	$[-10, 10]$
Push duration	$[2, 30]$

Table 5. Tunable hyperparameters and search space in the robot arm pushing task.

15.5. Rover Trajectory Planning

This task is a 60D problem, where our target is to optimize the trajectory of the rover, determined by our choices of 30 points, in a 2D plane. The reward is estimated in the following way:

$$f(x) = c(x) + \lambda(\|x_{0,1} - s\|_1 + \|x_{59,60} - o\|_1) + b,$$

where s and o are the starting position and the target position, $x \in [0, 1]^{60}$ containing the points picked, and $c(x)$ is a function to measure the cost of the trajectory determined by x .

Instructions for running these two tasks can be found in <https://github.com/uber-research/TuRBO> and <https://github.com/zi-w/Ensemble-Bayesian-Optimization>.